Dynamic Braking Of Induction Motors

Dissertation submitted in partial fulfilment of the requirements for the Degree of

MASTER OF ENGINEERING
IN
ELECTRICAL MACHINE DESIGN

By
S. RAMA KRISHNAN, B.E. (Hons.)

DEPARTMENT OF ELECTRICAL ENGINEERING
UNIVERSITY OF ROORKEE

C E R T I F I C A T E

CERTIFIED that the dissertation entitled DYNAMIC BRAKING OF INDUCTION MOTORS which is being submitted by Sri S. RAMA KRISHNAN in partial fulfilment for the award of the Degree of Master of Engineering in Electrical Machine Design of University of Roorkee is a record of the student's own work carried out by him under my supervision and guidance. The matter embodied in this dissertation has not been submitted for the award of any other Degree or Diploma.

This is further to certify that he has worked for a period of three months from June 15, 1962 to September 15,1962 for preparing dissertation for Master of Engineering Degree.

(D. R. KOHLI)

Reader in Electrical Engineering

Roorkee.

September 22,1962.

A C K N O W L E D G E M E N T S

The author wishes to express his profound sense of gratitude to Sri D.R. Kohli, M.E.E., (Cornell), Reader in Electrical Engineering for his valuable advice and suggestions at every stage of the preparation of this dissertation.

The author wishes to thank Prof. C.S. Ghosh for the various facilities afforded in the department in connection with this work.

Sincere thanks are also due to Dr. C.S. Jha, formerly Reader in Electrical Engineering and Dr. V.Ahmad, Development Officer, Ministry of Steel and Heavy Industries for their valuable help.

C O N T E N T S

S Y N O P S I S

The scope of this dissertation extends only to the dynamic braking of induction motors by d.c. injection. The various methods of analysis of the problem have been critically reviewed. A simplified method along with the associated set of equations, based on Cochran's method for the calculation of the d.c. braking performance of an induction motor is presented. This method is shown to give reasonable accuracy comparable with the existing methods of analysis. The most accurate existing method of analysis has been discussed first. The other methods are presented later with a discussion of their relative merits and drawbacks in the subsequent chapters. All the methods of analysis have been reduced to a standard form of equations for effective analytical comparison. Practical utility of the methods has been analysed and comparison with actual test results have been made by calculating the d.c. braking characteristics of two induction motors (one slip-ring and the other a squirrel-cage) by using all the methods. The test details of the motors concerned have been compiled from published works.

NOMENCLATURE

C = Induced voltage per phase per r.p.m.

E_2 = Induced rotor voltage per phase, volts, of unit angular frequency ω_s.

E_{2R} = Voltage drop across rotor resistance, volts, of unit angular frequency ω_s.

e_{2R} = Voltage drop across rotor resistance, volts, of slip frequency.

E_{2X} = Voltage drop across rotor reactance, volts, of unit angular frequency ω_s .

e_{2X} = Voltage drop across rotor reactance, volts, of slip frequency.

I_1 = Stator current, amps, of unit angular frequency ω_s.

I_2 = Rotor current, amps, of unit angular frequency ω_s.

I_d = Stator direct current, amps.

J = Moment of inertia of the rotating masses at motor shaft, pound- feet^2.

K = .000462 J .

m = Number of phases.

N_s = Synchronous speed corresponding to unit angular frequency ω_s , r.p.m.

N_2 = Rotor speed r.p.m.

P = Synchronous reactance per r.p.m, ohms/r.p.m.

•

R_1 = Stator resistance, ohms.

R_2 = Rotor resistance, ohms.

s = Slip under normal motoring operation ($s = \frac{\omega_s - \omega_2}{\omega_s}$)

S = Fractional slip under dynamic braking operation ($s = \frac{\omega_2}{\omega_s}$)

T = Torque, synchronous watts.

V_1 = Stator supply voltage per phase, volts.

V_2 = Rotor e.m.f. per phase at angular frequency ω_s , volts.

W_0 = Kinetic energy of drive at speed of N_s, joules.

W_1 = Energy loss in primary winding, joules.

W_2 = Energy loss in secondary circuit, joules.

X_1 = Stator winding leakage reactance per phase, ohms (frequency ω_s).

X_2 = Rotor winding leakage reactance per phase, ohms (frequency ω_s).

X_m = Magnetizing reactance per phase, ohms (frequency ω_s).

X_s = Synchronous reactance of rotor circuit per phase, ohms (frequency ω_s).

ω_s = Unit angular frequency or synchronous speed, electrical radians/second.

ω_1 = Stator supply angular frequency, electrical radians/second.

ω_2 = Rotor speed, electrical radians per second.

(I_1, I_2, R_1, R_2, V_1, V_2, E_{2R}, E_{2x}, X_1, X_2, X_m are all referred to the same winding)

The abbreviations, not mentioned above are individually explained as and when necessary.

INTRODUCTION

Retarding electrical machines either to a lower speed or to standstill is a normal requirement in their various applications. In some cases reversals of speed may also be warranted. Retardation of electric motors can be effected either by friction brakes or electrical braking.

A friction brake may consist of a brake shoe with friction lining, pressed on to a drum fixed on to the shaft of the machine, thereby converting the kinetic energy of the rotating masses into heat at the drum and this is the only reliable brake to hold the machine against any disturbing force though the shock produced in the system may be detrimental unless properly designed. The friction shoes can be controlled electromagnetically by means of a solenoid.

In contrast to the friction brake electrical braking has a distinct advantage of a smooth shockless operation. Electrical braking of induction motors can be broadly classified as

(1) D.C. braking
(2) A.C. braking

The second method can be further subdivided as

(a) Braking with excitation by capacitors
(b) Regenerative braking
(c) Plugging
(d) Braking by unbalanced operation.

In d.c. braking, the stator is switched off from the a.c. supply and connected across a source of direct current. This creates alternate north and south poles in the stator and the resulting flux induces an e.m.f. in the short-circuited rotor windings thereby circulating a current in them. A braking torque is thus obtained from these currents and the machine decelerates. Thus, the machine is acting as a generator of varying speed connected to a high power factor load. The braking characteristic is such that the braking action is not effective at very low speeds and consequently in the case of such loads as crane hoists etc. friction brake must be applied to hold the load stationary. This form of braking is widely used in various industrial applications such as lifts, mine-winders, machine tools, strip mills etc.

In the first mentioned method of A.C. braking schemes, suitably rated capacitors are connected across the stator terminals and when the machine is disconnected from the supply the capacitors excite the stator winding, and induction generator action is achieved. Also sometimes external resistances are connected to the stator winding to receive and dissipate the energy evolved, thereby reducing the stator heating. Practical applications of this rather expensive form of braking are limited because no braking torque is produced below about 1/3 of the synchronous speed.

Regenerative braking is the method of retarding the motor by making the motor function as a generator pumping the generated power back to the supply line. Lowering the applied frequency or increasing the number of poles results in the machine to run as a generator and feeds back the power to the supply. It may be noted that complete stopping of the motor by means of this method is not possible. Application of low frequency braking has been investigated for use in mine winders by Dixon and Tiley.[30]

Plugging is the method of retarding the motor speed and stopping or reversing the drive by the application of the electric power such that the motor develops torque in the opposite direction to that in which it is revolving. In the case of three phase induction motors this is simply achieved by interchanging two of the supply leads. The phase rotation of the stator magnetic flux is then reversed so that the motor is running at a negative speed with respect to the revolving stator field and the motor decelerates. Though a fast braking performance is achieved by a simple arrangement and installation this method of braking results in high energy consumption and consequent heating of the machine. Also a zero-speed switch or consistent timing relay is required if reversing is to be prevented.

Unbalanced operation of an induction motor can be performed by applying an unbalanced voltage to the stator winding, or by asymmetrical connection of the stator winding or introducing unbalanced external impedences in the rotor circuit. Any unsymmetrical 3-phase system can be transformed into three balanced systems by the application of the principle of symmetrical components, the positive sequence component providing a driving torque and the negative sequence component giving a retarding torque and the zero sequence component either or neither depending on the type of connection and the speed of the motor. By adjusting the extent of unbalance these torques can be varied for getting different torque-speed characteristics.

This type of speed control has been widely used in a number of industrial applications.

Having briefly mentioned the various electrical braking methods, it will now be appropriate to look into the aspect of defining "Dynamic braking". An exact definition of the term "Dynamic braking" as applied to induction motors is by itself a problem involving many controversial opinions. Apparently this term was originally used for d.c. shunt motors where the armature is switched off from the supply and a resistance connected across the same for braking.

In describing dynamic braking of Induction motors P.L.Alger[32] mentions that the term "dynamic braking" is applied to that mode of operation in which direct current is injected into the stator for braking. M.G. Say[34] also views the problem in the same way and specifies "dynamic braking" of an induction motor is achieved by exciting the stator winding from a d.c. source, and classifies "dynamic braking" as one of the methods of " electric braking ". Many authors including Karapetoff[35] take dynamic braking of induction motors as one in which d.c. excitation is used. Also there are quite a few authors like Butler[31], Srinivasan[36] and Ahmad[31] who imply and include plugging, regenerative braking capacitor braking and braking by unbalanced operation under the term "Dynamic braking", but a clear-cut definition has not been given.

Literally analysing the term "Dynamic" hardly leads us to support or oppose either opinion. Though a broader definition of the term "dynamic braking" to include all electrical braking s, is appealing, it would have been more so if the term ro-dynamic braking" were used, meaning that the braking is ed by electro-dynamic action.

The scope of this dissertation extends only to the : braking of induction motors by d.c. injection.

CHAPTER I

A RESUMÈ OF PUBLISHED WORK ON D.C. BRAKING OF INDUCTION MOTORS

CHAPTER I

A RESUMÉ OF PUBLISHED WORK ON D.C.BRAKING OF INDUCTION MOTORS

1.1. Principle of d.c.dynamic braking of induction motors.

In this method of braking, the stator of the motor is disconnected from the a.c.source, and a source of direct current is connected to it as shown in figure 1.1, the type of connection depending on the control and design features of the system. The direct current flowing through the stator winding will produce adjacent poles of alternate polarity, and a stationary magnetic field in space is established. As the rotor is revolving, an e.m.f. is induced in the rotor conductors and currents are circulated in the short-circuited rotor windings. The torque produced by the interaction of these rotor currents on the stator field, is in a direction opposite to the direction of rotation giving a braking action. Thus, the kinetic energy of the rotating masses is converted into electrical energy and dissipated as heat in the rotor winding. The machine decelerates to standstill.

1.2. Resumè of published work on d.c. dynamic braking.

The first published article on the use of direct current for dynamic braking of induction motors was put forward by Hellmond in 1910. The idea of converting direct stator current into equivalent alternating value depending on the type of stator connection to the

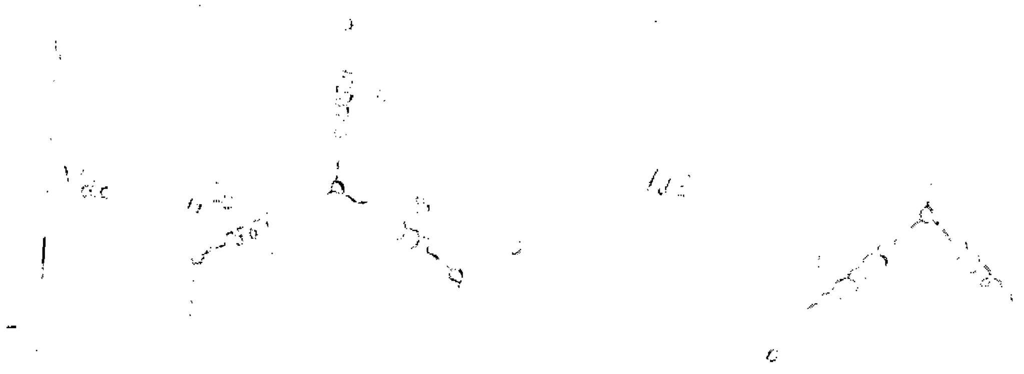

d.c. source was suggested in order to extend the transformer theory to this problem. Also a vector diagram of the theory of operation based on m.m.f. and flux considerations, taking saturation into account, was evolved from which the various performance characteristics were obtained making use of the design data. The approach is on sound theoretical basis, but very many cumbersome calculations are involved though the performance predictions can approach accuracy except for the fact that the harmonic effects are not considered, and the secondary reactance is neglected. In those days neglecting the secondary reactance was justified because of the fact that this type of braking was mainly used for slip-ring motors with external control resistance in the secondary and as such the secondary reactance was not much of a practical significance.

In the same year Rosenberg and Peck[2] commercialised this application and registered their patent in Britain.

There was a rather wide gap for more interest to be evinced on the subjec t which was mainly due to its restricted applications in practice. The momentum of industrial expansion invoked the latent interest in the problem in the 1930's when this form of braking found its place in steel industry and mines. Weissheimmer[3] put forward a method to find out the maximum torque value, and Harrel and Hough[4] presented a paper on the subject in 1935. The authors[4] gave empirical curves which were based on test results conducted on a wide range of squirrel cage motors. These curves were to help the designer for approximately calculating the direct current and wattage required for braking a given load in a given time. Hellmond[5] in a discussion of the above paper pointed out that all the characteristics obtained by the authors based on test results could be calculat from design data as well, and further extended the scope of his earlier publication to include the effect of secondary reactance in the performance. This was a complete and reasonably accurate prediction of the performance from design data but again involved laborious calculations. As a matter of fact the electrical aspect involved in the problem was completely solved and it was a question of finding an easier graphical or mathematical solution of the problem.

Bendz[7], in his paper in 1938 compared the various methods of braking an induction motor inclusive of d.c. dynamic braking. He also gave empirical curves based on test results for evaluating the direct current and wattage for stopping a particular drive in a given time, knowing the starting torque and rated current of the machine.

In the same year the application of d.c. dynamic braking for mine winders was described by Worrel[6] giving the typical characteristics.

LaPierre and Metaxas[13] approached the problem with the alternator theory considering the machine under d.c. braking as a short circuited alternator supplying a high power factor load, and evolved approximate torque/speed curves by the adjusted synchronous reactance method. But the discrepancies of the calculated and actual torques in the maximum torque region was explained off as that produced by tooth harmonics and an equation was given for the same. Definitely a harmonic induction torque is produced due to the presence of slots in the stator and rotor but not to the extent expressed. The very application of the Synchronous Impedence method as applied to alternators for solving the problems of dynamic braking of an induction motor is questionable because this method has never given consistent results and cannot properly take into account the excessive peaks of saturation reached in the motor under braking conditions along with a continuous change of frequency of the rotor circuit current. Thus, it is not surprising that the test results did not agree with those calculated on the basis of this method.

Cochran[15], in presenting his method applied to wound rotor induction motors also viewed the problem in the same way but used the zero power factor characteristic method for calculations which was based on design data. His method has not been compared with test results for an existing machine. Apparently the way in which the paper was presented has not attracted subsequent workers on the subject to utilise the method proposed. Anyway calculations made in this dissertation based on a modified form of Cochran's method, have shown that the method is reasonably accurate.

An equivalent circuit for dynamic braking operation and its application to find out the approximate torque value neglecting secondary reactance, along with a detailed description of a mine winder scheme, incorporating a slip ring motor was presented by Friedlander[9] in 1949.

Mulligan[16] gave a simple method of reasonable accuracy based on the standard circle diagram of the induction motor. But

•

Harrison[11] had given a simple graphical solution on the basis of a simplified equivalent circuit for dynamic braking conditions, for a slip ring motor neglecting secondary reactance. In 1955, in extending the scope of his earlier paper Harrison[20] published a reasonably accurate and simple graphical solution of the problem with the effect of secondary reactance taken fully into consideration. But this again could not be directly applied to all types of motors because the iron and stray losses and losses caused by space harmonic m.m.f's have not been taken into account. He also pointed out how inaccurate it is to take the average value of the torque over a speed range for calculating the running down time and made it clear that it is the average of the inverse of torque that affects the time; which can be quite different from that based on average torque especially for the nature of the characteristic obtained for dynamic braking.

Butler[22] showed that a mathematical rather than a graphical solution of the equations presented by Harrison, is possible and the various effects of saturation on the dynamic braking characteristics were analysed in detail. He also extended the method to include a wide range of calculations to evolve maximum torque, stopping time and energy losses[24] etc. The same theory was applied to double cage motors by Butler and Abdel-Hamid[25]. The authors point out that the speed/torque characteristic of a double cage motor under braking conditions is not similar to the slip/torque characteristic when motoring, as is the case for an ordinary induction motor, with normal value of rotor resistance and reactance. As the saving in the running down time will be as high as 50% in the case of the double cage motors, it was suggested that this can be taken advantage of, in frequent start-stop drives. Also, it was established that stray losses play an important role in contributing towards the braking torque in the case of double cage motors.

This method of braking of the induction motors has captured its place in a very wide range of industrial applications and is being increasingly used in various industries such as machine tools, steel mills, mines, paper mills etc.

CHAPTER 2

MACHINE PERFORMANCE UNDER D.C. DYNAMIC BRAKING CONDITIONS-INDUCTION MOTOR APPROACH OF ANALYSIS

2.1. An analogy of the induction motor under normal motoring operation, and under d.c. dynamic braking.

2.2. Equivalent circuit.

2.3. Performance equations for d.c. braking.

2.4.1. Dynamic braking conditions-the inevitable presence of magnetic saturation.

2.4.2. The treatment of saturation in the analysis.

2.4.3. Determination of the open-circuit characteristic.

2.5. The nature of the parameters - secondary resistance, and reactance, in the performance equations.

2.6. Conditions for maximum torque.

2.7. Prediction of performance characteristics for dynamic braking conditions.

2.8. Graphical determination of the characteristics.

2.9. Nature of the braking characteristics.

2.10. Stopping time under d.c. braking.

2.11. Energy losses under d.c. braking.

CHAPTER 2

MACHINE PERFORMANCE UNDER D.C. DYNAMIC BRAKING CONDITIONS INDUCTION MOTOR APPROACH OF ANALYSIS

2.1. An analogy of the Induction Motor under normal motoring operation, and the machine under d.c.braking.

The motor supplied from its normal a.c. source, at stand still, has a rotating field having the synchronous speed N_s, with respect to the rotor at that instant. This can be viewed as similar to a condition when the stator field is at standstill excited by a direct current, to produce the same intensity of the field, and the rotor revolving at synchronous speed N_s, thus having the same relative speed. In the same way the rotor revolving at (almost) the synchronous speed from the a.c. supply is similar to the condition of a d.c. excited stator winding with the rotor at rest. Thus the conditions with the slip s under normal motoring is similar to the slip (1 - s) for the braking operation. This is the first analogy that helps to view the d.c. braking operation of an induction motor. Thus the stator direct current can be transformed into an equivalent alternating current and the performance can be analysed as for normal motoring operation provided the effect on the various parameters under this changed condition of operation is given due consideration in the various calculations. Hence, an induction motor under d.c. braking conditions can be suitably represented as one under motoring and the various factors developed for normal operation can be modified to meet the dynamic braking performance. This method[20,22] has been successfully applied to get valid results under braking conditions.

2.2. Equivalent Circuit.

The performance calculations of an induction motor can be usually based on an equivalent circuit, which can be developed step by step for the normal running of the motor. One phase of a polyphase induction motor can be represented as shown in figure 2.1 assuming a balanced symmetrical operation and neglecting the effect of the space harmonic magnetomotive forces and iron and stray losses.

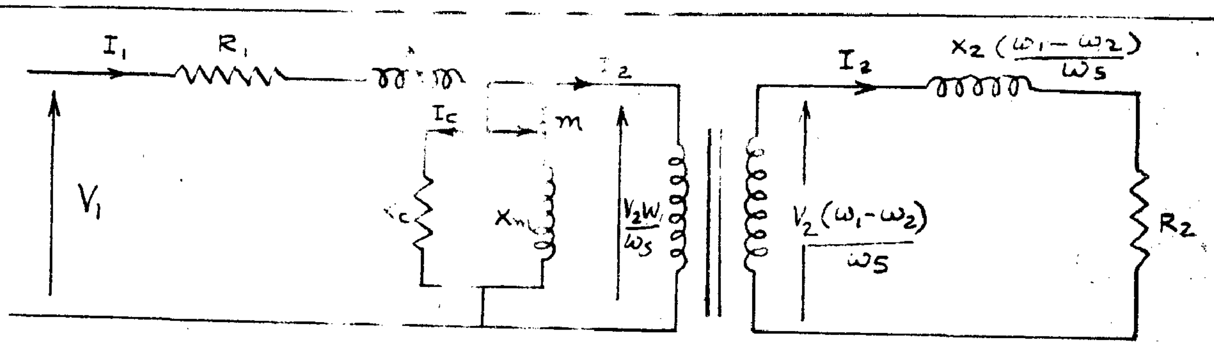

FIG. 2.1

THE EQUIVALENT CIRCUIT OF ONE PHASE OF A POLYPHASE INDUCTION MOTOR. THE STATOR VOLTAGE FREQUENCY IS ω_1 AND THE ROTOR FREQUENCY IS $(\omega_1 - \omega_2)$. THE QUANTITIES V_2, X_1, X_2 AND X_m ARE ALL REFERRED TO ANGULAR FREQUENCY ω_s.

It may be noted that in the equivalent circuit shown in the figure 2.1, the quantities V_2, X_1, X_2 and X_m are all based on a unit angular frequency ω_s electrical radians/second, which is the frequency for normal operation and normal synchronous speed. The stator applied voltage is V_1 volts and is having a frequency of ω_1 electrical radians/second. The stator winding which is known as the primary of the induction motor, is shown as an ideal primary winding AB in series with a resistance R_1 and a constant leakage reactance $X_1 \frac{\omega_1}{\omega_s}$ and the induced e.m.f. in the primary is $V_2 \frac{\omega_1}{\omega_s}$ volts.

The rotor winding is assumed to be perfectly coupled with that of the stator and the magnetizing and core loss components of the current are represented by the parallel paths X_m and R_c, across the terminals (A, B) of the ideal primary winding. The rotor can be represented as a perfect winding CD assumed to have a 1:1 turn ratio with the primary, and having a voltage $\frac{V_2 (\omega_1 - \omega_2)}{\omega_s}$ induced at its terminals CD by the mutual flux and having the resistance R_2 and reactance, $\frac{X_2 (\omega_1 - \omega_2)}{\omega_s}$ external to the ideal winding.

Fig. 2.1 cannot be directly dealt with like a simple electrical circuit because the ideal primary and secondary windings are not electrically interconnected, even though they are magnetically coupled. In order to interconnect them electrically, the terminal voltages across the ideal primary and secondary windings are to be made equal, and they should be at the same unit angular frequency ω_s ; and this is to be accomplished without changing the magnitudes and phase angles of the respective currents. This is achieved by dividing the voltages, resistances and reactances of the primary side by $\frac{\omega_1}{\omega_s}$; and those on the secondary side by $\frac{\omega_1 - \omega_2}{\omega_s}$. The primary side and secondary side can now be combined as shown in fig. 2.2 in which the angular frequency throughout is ω_s.

Analysing the circuit under the conditions of d.c. dynamic braking, the stator applied voltage is direct and hence $\omega_1 = 0$.

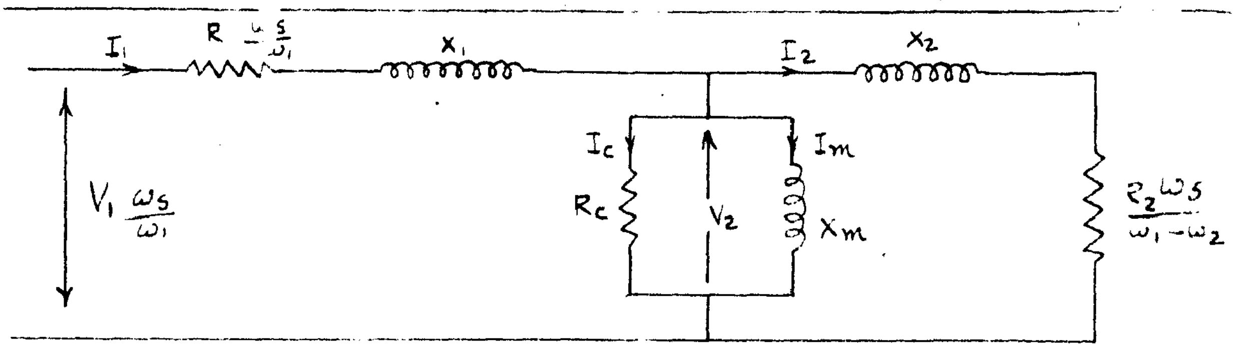

FIG. 2.2

FULLY DEVELOPED EQUIVALENT CIRCUIT OF ONE PHASE OF A POLYPHASE INDUCTION MOTOR.

Thus, the stator applied voltage and stator resistance become infinite which exactly corresponds to the conditions assumed in the application of Thevenin's theorem for a constant current to the circuit. Thus the stator resistance and applied voltage need not be shown in the equivalent circuit for the d.c. braking operation. It should be kept in mind that I_1 is an alternating current of angular frequency ω_s electrical radians per second, which is electromagnetically equivalent to the direct current injected into the stator winding. The equivalent alternating current corresponding to a given d.c. value, will depend on the type of connection envisaged for exciting the winding, shown in figure 1.1. Nearly sinusoidal wave shape of the field, will be obtained by all the connections mentioned, as the poles are of non-salient type with distributed winding. The currents flowing in each of the four connections can be considered to represent different instants of time on a 3-phase input current wave. Thus in figure 1.1a current in phase A is having the peak-value, whereas currents in phases B and C are at half the values. Thus equating the currents, we get,

$$I_D = I_{max} = \sqrt{2}\ I_1$$

where I_D is the direct current, I_{max} the maximum value of the equivalent alternating current and I_1 its effective value. Thus $I_1 = \dfrac{I_D}{\sqrt{2}}$ in the first case.

Similarly it can be shown that I_1 is equal to $\dfrac{\sqrt{2}}{\sqrt{3}} I_D$, $\dfrac{\sqrt{2}}{3} I_D$ and $\dfrac{1}{\sqrt{6}} I_D$ respectively for the connections b, c and d shown in fig. 1.1.

Now for $\omega_1 = 0$, the rotor resistance becomes $R = -\dfrac{\omega_s}{\omega_2} R_2 = -\dfrac{R_2}{S}$ where S is the fractional speed given by $S = \dfrac{\omega_2}{\omega_s} = \dfrac{N_2}{N_s}$. The negative sign shows that a braking torque is produced. It can be seen that $S = 1 - s$, where, s is the slip for normal operation as a motor given by $s = \dfrac{N_s - N_2}{N_s}$.

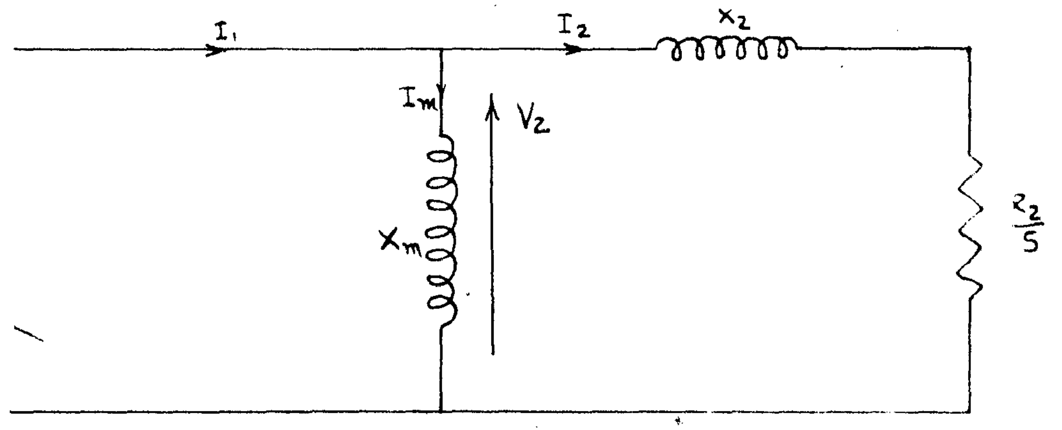

FIG 2·3

EQUIVALENT CIRCUIT OF ONE PHASE OF A POLYPHASE INDUCTION MOTOR UNDER D.C DYNAMIC BRAKING. I_1 IS THE EQUIVALENT ALTERNATING CURRENT CORRESPONDING TO THE DIRECT CURRENT.

Having determined to inject a controlled value of direct current of required magnitude, the stator reactance need not be shown. Also the core loss component R_c disappears which is fully justified because actually a direct current is flowing in the winding. Thus the equivalent circuit can be further simplified as shown in fig. 2.3.

At this stage it is necessary to make it perfectly clear that analysis of motor operation, through the equivalent circuit is a matter of convenience. All the performance equations can be directly derived from energy considerations. Even if an equivalent circuit was desired it could have been derived directly for dynamic braking conditions without viewing it first as an ordinary induction motor. But as it is felt that a common approach to both the problems will much better, this procedure[20] is preferred.

2.3. Performance equations.

The performance equations can now be derived from the equivalent circuit as follows. Referring to figure 2.3,

$$I_1 = I_m + I_2 \qquad 2.1$$

$$V_2 = I_m \, j \, X_m = I_2 \left(\frac{R_2}{S} + jX_2 \right) \qquad 2.2$$

From equations 2.1 and 2.2.

$$I_1 = \frac{I_2 \left[\frac{R_2}{S} + j \left(X_2 + X_m \right) \right]}{j \, X_m} \qquad 2.3$$

Equation 2.2 gives

$$V_2^{\,2} = I_m^{\,2} \, X_m^{\,2} = I_2^{\,2} \left[\left(\frac{R_2}{S} \right)^2 + X_2^{\,2} \right] \qquad 2.2a$$

from which

$$\frac{R_2}{S} = \sqrt{\frac{V_2^{\,2}}{I_2^{\,2}} - X_2^{\,2}} \qquad 2.4$$

Equation 2.3 gives

$$I_1^{\,2} = \frac{I_2^{\,2} \left[\left(\frac{R_2}{S} \right)^2 + \left(X_2 + X_m \right)^2 \right]}{X_m^{\,2}} \qquad 2.3a$$

Substituting equation 2.4 in the above and solving we get

$$I_2 = \sqrt{\frac{I_1^{\,2} - I_m^{\,2}}{1 + 2 \frac{X_2}{X_m}}} \qquad 2.5$$

Substituting equation 2.5 in 2.4 we get,

$$\frac{R_2}{S} = \sqrt{\frac{I_m^2 \, (X_2 + X_m)^2 - I_1^2 \, X_2^2}{I_1^2 - I_m^2}} \qquad 2.6$$

But we know $S = \frac{N}{N_s}$ from which the speed N can be calculated. The torque in synchronous watts will be

$$T = m. \, I_2^2 \, \frac{R_2}{S} = m. \frac{I_1^2 \, X_m^2 \, (\frac{R_2}{S})}{(\frac{R_2}{S})^2 + (X_2 + X_m)^2} \qquad 2.7$$

where m is the number of phases in the machine.

In deriving the equivalent circuit and hence the above equations, it has been made clear that the effects of iron and stray losses and those due to the space harmonic m.m.f's have not been taken into account. But they are usually negligible for an ordinary induction motor. Also the friction and windage losses cannot be considered in the equivalent circuit. Subject to these limitations all the equations 2.1 to 2.7 hold good provided proper values of the parameters R_2, X_2 and X_m are substituted keeping in view the changed conditions of operation under dynamic braking.

2.4.1. D.C. Dynamic Braking Conditions- the inevitable presence of saturation.

Normally the design of an induction motor is such that the magnetizing current is as small as possible, and for normal motoring operation of the machine, saturation of the magnetic circuit does not set in. This will be evident from a comparison between the magnetizing current and the rated current giving rated torque, for normal machines. The value of the magnetizing current will be found to be only of the order of about one third of the rated stator current for a normal motor.

But the conditions under d.c. dynamic braking are very different. As the machine decelerates during braking, from the speed at which it was running towards standstill, the magnitude of the rotor current is decreased from a maximum value to zero towards standstill. The value of the stator current is constant because a constant direct current is injected into the stator. Thus from equation 2.5 it follows that the magnetizing current is increased as the speed decreases and equals the stator current I_1 at standstill. The above statement can also be elaborated, from the physical reactions taking place in the machine. At higher values of speed, as the rotor current is high, the demagnetizing effect of the rotor current on the stator flux is quite high and the machine will be operating under unsaturated magnetic conditions, for normal values of the rotor resistance. As the machine slows down the demagnetizing effect is progressively decreased and is zero at standstill. Thus even if the direct current injected is that corresponding to the normal rated current, values of magnetizing current three times that for the normal conditions of operation will result.

Unfortunately the application of the rated values of the direct current does not provide the necessary braking torque required in majority of the practical applications. A direct current equivalent to the rated alternating value gives a maximum torque of only about 70 to 90% of the full load torque for normal machines, and the average torque will be very much less (which will be evident from the shape of the torque/speed curve Fig.2.7). This seldom meets the minimum requirements of the braking performance. It is evident from equation 2.7 subject to the absence of saturation (i.e., X_m constant) that the torque is proportional to the square of the stator current I_1 for a particular value of speed i.e. doubling the value of exciting current will yield a torque four times the previous value. But if saturation is present, such a proportional increase in the torque cannot be achieved (because the value of X_m in equation 2.7 will then decrease). Thus it becomes all the more necessary, to increase the excitation further, to get an increased torque value. In normal practice one to four times the rated value has to be used in many applications. Thus we see that the magnetizing current as high as 3 to 12 times that required for normal operation can result, if the injected direct current is kept constant all through the speed range. Hence excessive peaks of saturation in certain regions of the torque/speed characteristic are bound to occur.

2.4.2 Treatment of Saturation in the analysis.

As per the equivalent circuit shown in fig.2.3, the magnetizing current is assumed to be determined by the resultant air gap flux inducing the air gap voltage V_2. As such the value of magnetizing current corresponding to a specified value of air gap voltage V_2 is assumed to be the same for all operating conditions. This assumption is undoubtedly valid for unsaturated magnetic conditions and is equally applicable for saturated conditions as well, if the effects of the various leakage fluxes on the saturation of stator and rotor iron are neglected. Omission of these effects, which are comparatively small is justified. Thus, the representation of the induction motor performance through the equivalent circuit shown in figure 2.3, makes the handling of saturation which is largely a complex magnetic circuit problem, into a comparatively simple engineering proposition. Evidently the magnetization curve forms the connecting link between the electric and magnetic circuit aspects. In the case of an induction motor the magnetization curve is in the form of an open circuit characteristic which can be interpreted as the relationship between the magnetizing current I_m and the air gap voltage V_2. Thus, the magnetizing reactance X_m which is a fictitious reactance introduced into the equivalent circuit, is directly defined by the open circuit curve, as the ratio $\frac{V_2}{I_m}$ at any point. Under unsaturated conditions X_m will be a constant X_{mu} equal to the initial slope of the open circuit characteristic. In the presence of saturation depending on the value of V_2, corresponding values of X_m as determined by the open circuit curve are to be used in solving the equations 2.1 to 2.7.

2.4.3. <u>Determination of the open circuit characteristic.</u>

As applied to the alternator the open circuit characteristic is the curve showing the relationship between the d.c. exciting current and the terminal voltage per phase of the open circuited armature, the machine being driven at the normal synchronous speed. As applied to the induction motor, it can be defined as the relationship of the magnetizing current I_m and the air gap voltage V_2. The induction motor can be coupled to a d.c. motor and can be driven at the synchronous speed. An a.c. variable voltage normal frequency 3-phase supply is then switched on to the induction motor The speed of the machine is then adjusted slightly if required such that the a.c. current input is a minimum. The voltage and current supplied are then noted down. By varying the applied voltage a set of readings can be taken.

As the power factor will be very low the airgap voltage can be found by directly subtracting the stator leakage reactance drop from the applied voltage giving

$$V_2 = V_1 - I_1 X_1$$

As the machine is driven at the synchronous speed the rotor currents will vanish and hence I_1 is the magnetizing current, inducing the air gap voltage V_2.

It may be noted that results of reasonable accuracy can be obtained even without driving the induction motor by external means. The motor running freely from the a.c. supply, on no load, will have only very small rotor current which can be neglected.

Also the open circuit curve can be predicted[15] from design data as well, which is exactly similar to that applied in alternator calculations.

2.5. The nature of parameters R_2 and X_2 involved in equations 2.1 to 2.7

Secondary Resistance R_2

Under d.c. braking conditions, the frequency of the rotor current varies continuously from almost the line frequency near the synchronous speed to a very low value towards standstill. In fact zero frequency of rotor currents never exists as the rotor currents will then be zero. A variation in the effective rotor resistance R_2 can be expected during the braking operation. A

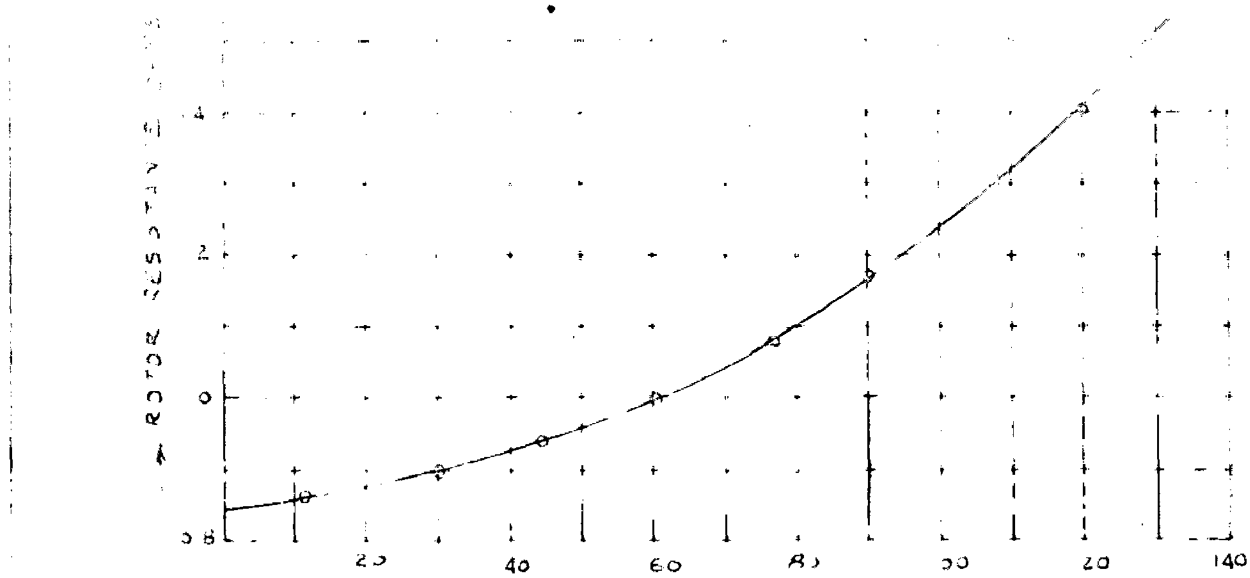

FIG. 24

FIGURE SHOWING THE VARIATION OF RESISTANCE WITH FREQUENCY FOR AN ORDINARY SQUIRRELCAGE INDUCTION MOTOR (REFERENCE NO. P 467)

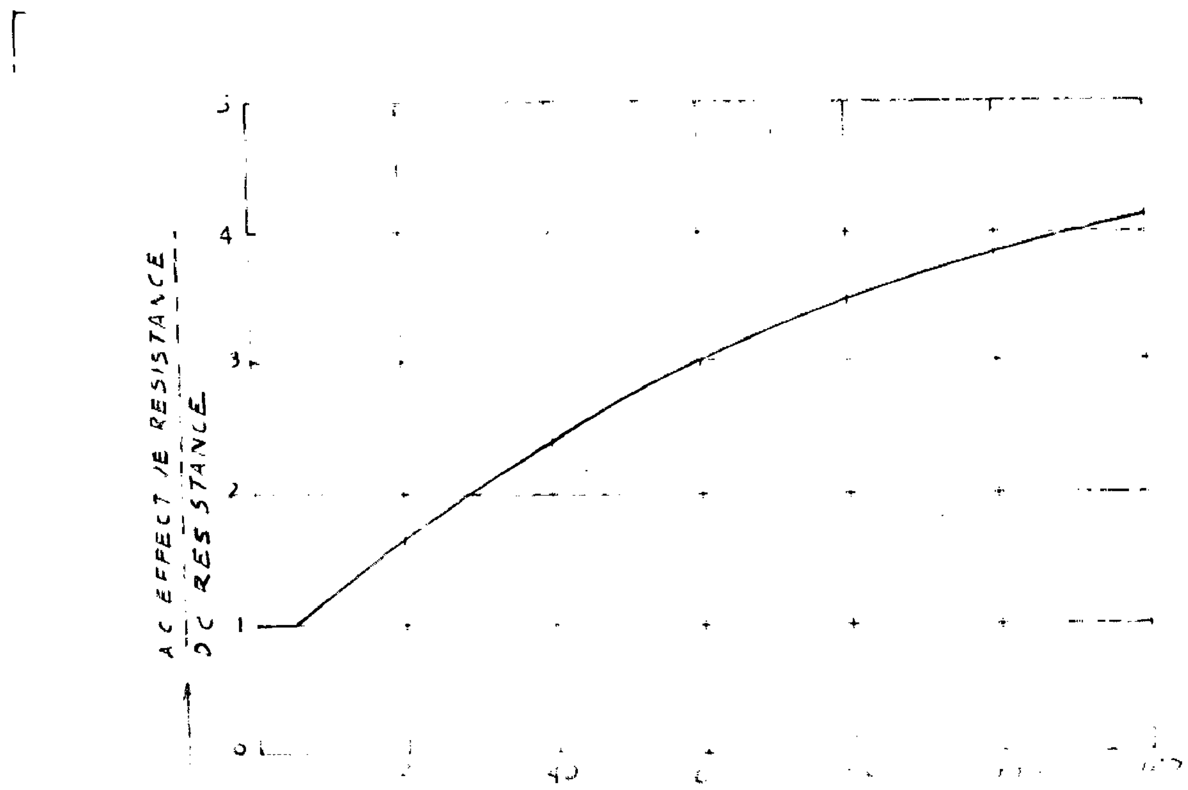

FIG. 25

CURVE SHOWING THE VARIATION OF EFFECTIVE RESISTANCE WITH FREQUENCY, DUE TO THE SKIN EFFECT IN COPPER ROTOR BAR (DEEP) (REF. , P 4) curve showing the variation of the secondary resistance with frequency can be plotted and can be used along with equations 2.1 to 2.7 for the performance prediction, which will invariably involve a trial and error procedure. Such a curve[28] showing the resistance variation with frequency, for a normal induction motor is shown in figure 2.4 and the curve[33] for motors of special construction such as deep bar and double cage motors are shown in figure 2.5. It can be readily seen that for the latter case the variation is much pronounced and as such this complex variation of the effective resistance with speed has to be suitably accounted for. But in case of an ordinary induction motor the variation is not so wide and most of the authors[20,22] have taken the effective resistance R_2 at the normal frequency and have used the same for performance calculations getting results of reasonable accuracy.

Secondary Reactance X_2

It should be stressed that according to the equivalent circuit fig. 2.3 the secondary reactance is always based on the unit angular frequency ω_s. The secondary inductance can vary with the varying frequency and the changed magnetic conditions, when the speed of the machine decreases. Usually the variation of the secondary inductance of an ordinary induction motor is negligible. In the case of a wound rotor induction motor with external secondary resistance the effect of even secondary reactance itself is not prominent as compared to the large secondary resistance. Under d.c. braking conditions, as the machine slows down, the effect of the secondary reactance on the characteristics is further reduced for decreasing values of speed. Thus, only for motors of special construction such as deep bar and double cage motors, the rotor reactance has to be considered as a complex function of speed and has to be suitably accounted for.

2.6. Conditions for maximum torque.

If there were no saturation a simple solution to compute the value of the maximum torque can be readily arrived at, because under unsaturated conditions X_m is constant at a value X_{mu}, which is the initial slope of the open circuit characteristic.

Thus for unsaturated conditions equation 2.7 gives

$$T = m. \frac{I_1^2 \quad X^2_{mu} \quad (\frac{R_2}{S})}{(\frac{R_2}{S})^2 + (X_2 + X_{mu})^2} \qquad 2.7.a$$

Differentiating the above expression with respect to $(\frac{R_2}{S})$ and equating the derivative to zero, we get the condition for the maximum torque. This will reduce to the form

$$\frac{R_2}{S} = X_2 + X_{mu} \qquad 2.8$$

and the value of the maximum torque will be

$$T_{max} = \frac{I_1^2 \quad X^2_{mu}}{2 \ (X_2 + X_{mu})} \qquad 2.9$$

Thus, it can be seen that the value of the maximum torque is independent of R_2 if saturation is absent.

But the effect of saturation is considerably pronounced (Ref. article 2.4) under dynamic braking conditions and as such cannot be neglected. The maximum torque under these conditions cannot be directly expressed in a mathematical form due to the involvement of the magnetization curve which has no linear equation. The best solution under these conditions is graphical and the maximum value of the torque has to be obtained after plotting the torque/speed characteristic. Cumbersome calculations[22] involving the slope of the magnetization curve (which is a variable) have been presented, which is more laborious than plotting the torque/speed curve, because a cut and try procedure is invariably involved in effecting a calculation.

An approximate location of the region of the maximum torque will aid in choosing different points to draw the torque/speed curve in the region where the maximum torque occurs, from which the accurate value of the maximum torque and speed at which this occurs can be found out.

In order to approximately determine the maximum torque and the speed at which this occurs, let us neglect X_2. Then the equation for torque can be written as

$$T = m.\ V_2\ I_2 \quad (\because \text{ the secondary power factor is unity})$$

By differentiating the above with respect to I_2 and equating to zero, we get the condition for maximum torque.

$$\frac{dT}{dI_2} = m\left(V_2 + I_2 \frac{dV_2}{dI_2}\right) = 0$$

Hence $$\frac{dV_2}{dI_2} = -\frac{V_2}{I_2}$$

But $$I_2^{\,2} = I^2{}_1 - I_m^{\,2} \quad \text{(From equation 2.5 because } X_2 = 0\text{)}$$

Differentiating both sides of the above equation with respect to I_2 we get

$$2I_2 = -2I_m \frac{dI_m}{dI_2} \qquad \text{(b)}$$

From equations (a) and (b) it follows that the maximum torque occurs at a point P on the open circuit characteristic such that

$$\left(\frac{dV_2}{dI_m}\right)_P = \left(\frac{V_{2p} \; I_{mp}}{I_1^2 - I_{mp}^2} \right) \qquad 2.10$$

where V_{2p} and I_{mp} are the values of V_2 and I_m at the point P on the open circuit curve, and $\left(\frac{d\,V_2}{dI_m} \right)$ is the slope of the open circuit curve at point P.

The point P is located by a trial and error procedure. Then values of I_m close to I_{mp} are chosen to draw the torque/speed curve (as described in section 2.7) from which the correct value of the maximum torque and the speed at which this occurs can be found out.

It may be noted from equations 2.8 and 2.9, that an increase in the secondary reactance is only going to decrease the maximum torque and is going to increase the speed at which this occurs. Keeping this in view values of I_m less than I_{mp} can be chosen to draw the torque/speed curve in the region of the maximum torque, for an accurate determination of the maximum torque value.

2.7.1. Prediction of torque/speed characteristics for a normal 3-phase induction motor undergoing d.c. dynamic braking.

As discussed already the secondary resistance R_2 and reactance X_2 , will be assumed to be non-varying parameters independent of frequency. A particular value of the direct current I_D is chosen. The corresponding equivalent alternating current I_1 can be immediately found out depending on the type of connection of the stator winding to the direct current source as explained in article 2.2. Assuming any value of I_m (which should be naturally less than I_1) the induced voltage V_2 is found out from the open circuit characteristic of the machine at synchronous speed. The value of X_m for that particular value of I_m is then given by $X_m = \frac{V_2}{I_m}$. Substituting the values of I_1, I_m and X_m in equations 2.5 to 2.7, the values of the secondary current, the torque and the speed can be determined. From the values obtained the torque/speed curve can be plotted. The results can be tabulated as shown in Table No. 2.1.

TABLE NO. 2

TABULAR FORM FOR PREDICTING SPEED TORQUE CHARACTERISTICS OF AN INDUCTION MOTOR UNDER D C BRAKING

QUANTITIES ASSUMED TO BE FIXED AND THEIR VALUES	LOAD POINTS	I_m	V_2	X_m	I_2	T	N
	1						
	2						
I_D =	3						
I =	4						
	5						
Z_2 =	6						
X_2 =	7						
	8						
	1						
	2						
I_D =	3						
I =	4						
	5						
Z_2 =	6						
X_2 =	7						
	8						

2.7.2. Prediction of the torque/speed curves for different values of I_D.

As before, the torque/speed curves for different values of the stator direct current I_D can be determined and the tabula-tion extended as shown in Table No.2.1.

2.7.3. Prediction of the torque/speed curves for different values of the secondary resistance.

The stator direct current is taken to be fixed at a particular value I_D. Hence, I_1 is also fixed. Now for any assumed value of I_m, equation 2.5 shows that the value of the secondary current I_2 is independent of R_2. Hence from equation 2.7 we can obviously conclude that for particular values of I_1 and I_m, the torque is directly proportional to $\frac{R_2}{S}$. Thus once the torque/speed curve for a set of particular values of I_1, X_2 and R_2 have been derived, the characteristic keeping I_1 and X_2 same as before, and R_2 increased to say R_3 can be obtained by shifting the former curve parallel to the speed axis by the ratio $\frac{R_3}{R_2}$. Or the same curve can be used by multiplying the scale of the speed axis by $\frac{R_3}{R_2}$.

2.7.4. Determination of the torque/resistance curves.

In certain applications such as automatic mine winders using slip ring motors the problem of keeping stable braking operation is better investigated by a set of torque/resistance curves at fixed values of the speed and excitation.

For determining the torque/resistance characteristics the quantities I_D and hence I_1, N_2 and X_2 are assumed to be fixed. The calculations are exactly the same as before except that the speed is assumed to be constant along with the fixed values of I_1 and X_2. Then for different assumed values of I_m, the values of the torque T and the secondary resistance R_2 are determined. The results can be tabulated as before, except that, the fixed value of N_2 is entered. in the first column, and the values of R_2 are noted down in the last column.

2.7.5. Prediction ofthe torque/resistance curves for different values of speed.

Equation 2.5 shows that for particular values of I_1 and I_m , the secondary current I_2 is independent of the speed. Hence for fixed values of I_1 and I_m the torque is directly proportional to $\frac{R_2}{S}$. Therefore, once the torque/resistance curve for particular values of N_2, I_1 and X_2 are determined, the curve for the same values of I_1 and X_2 and a different value of speed say N_3 is readily obtained by shifting the former curve along the resistance axis by the ratio $\frac{N_3}{N_2}$. Alternatively the same curve can be used by multiplying the resistance scale by $\frac{N_3}{N_2}$.

2.8 Graphical determination of the characteristics.

In the previous article, the performance characteristics have been evolved mathematically by using the equations 2.1 to 2.7 along with the open circuit curve of the machine. The same results can be obtained graphically as well, though subject to graphical error.

Referring to figure 2.6 , OM is the open circuit characteristic of the machine. Suppose it is required to determine the braking characteristics for a particular value of I_1, an arc is drawn as shown, with O as centre, and I_1 as the radius. The scale of

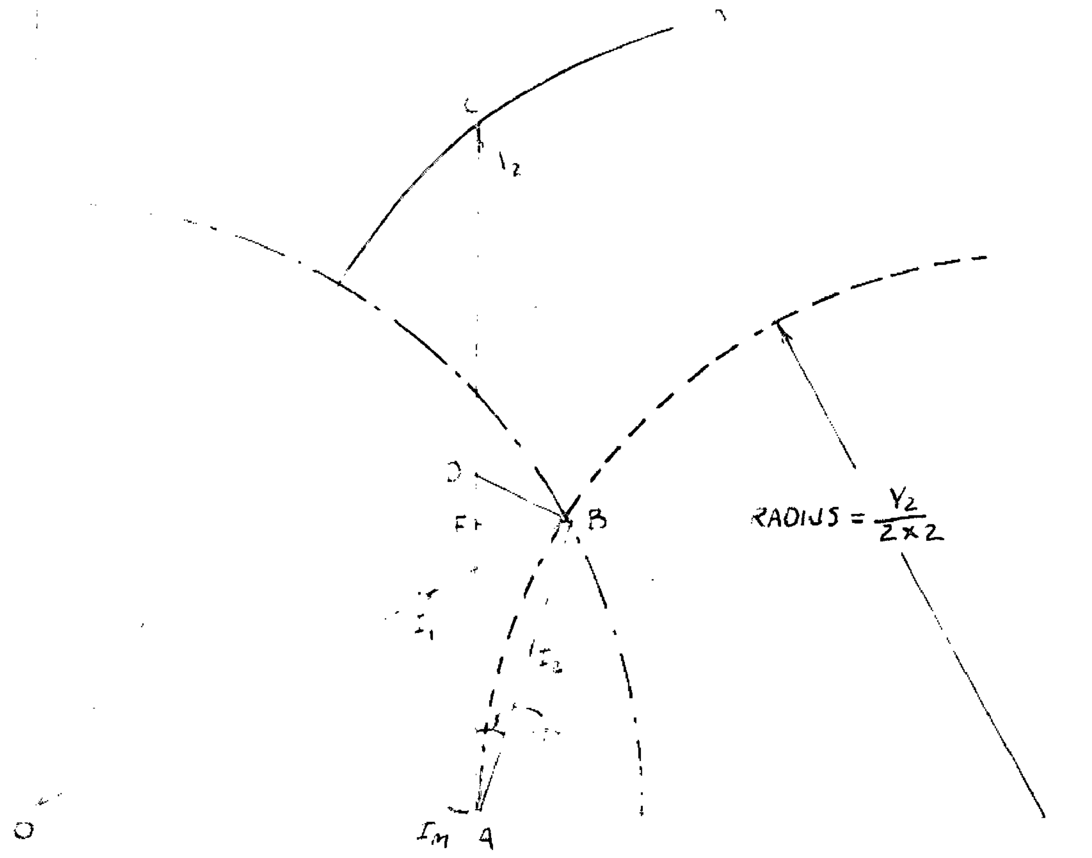

FIG 2 b

FIGURE SHOWING THE GRAPHICAL CONSTRUCTION TO DETERMINE THE TORQUE-SPEED CURVE OF AN INDUCTION MOTOR UNDER D C DYNAMIC BRAKING. O M IS THE OPEN CIRCUIT CHARACTERISTIC OF THE MACHINE AT SYNCHRONOUS SPEED.

I_1 should be the same as that used for drawing the curve OM. A value of $I_m = OA$ is now assumed ($I_m < I_1$). The point P is located on the line OAP such that $AP = \frac{V_2}{2\,X_2}$. From the equivalent circuit as shown in figure 2.3, it is evident that the locus of I_2 is a semi-circle with P as centre and a radius equal to $\frac{V_2}{2\,X_2}$, as shown in figure 2.6. As I_1 should be the resultant of I_m and I_2, the point of intersection B of the two circles, should give the value of I_2 both in magnitude and direction. Thus $AB = I_2$. AC is the value of V_2 for a magnetizing current equal to OA, and the CAB $= \phi_2$, which is the phase angle between the voltage and current of the secondary circuit.

Drop a perpendicular BF to the line AC. Also erect a perpendicualr at B on the line AB to cut AC at D. Then the torque

$$T = m.\ V_2\ I_2 \cos \phi_2$$
$$= m \times AC \times AF$$

where AC is measured in volts and AF is measured on the ampere scale.

Also, $\frac{R_2}{S} = \frac{AC}{AD} = R_2\ \frac{N_s}{N}$ from which the speed N is obtained.

The above construction is repeated for various values of I_m and the torque/speed characteristic can be readily plotted.

In an exactly similar way the torque/speed curves for various values of I_1, as well as torque/resistance characteristics can be obtained.

It is worthwhile point out, that in this particular method a direct mathematical analysis by using equations 2.1 to 2.7 is possible to get the braking characteristics, without involving any trial and error procedure. Hence the mathematical analysis is definitely preferable to the graphical method, because the latter method is always subject to graphical error.

2.9.1. The nature of the torque/speed characteristics under d.c. dynamic braking conditions.

The type of torque/speed characteristic obtained under d.c. dynamic braking conditions, of an induction motor is shown in fig. 2.8 curve A, for a short circuited rotor (i.e. without any external secondary resistance). The curve B shows the characteristic for normal motoring operation without any external secondary resistance. These curves have been compiled from the test data presented by Harrison[22] and Butler[24]. The details of the motor tested are given in Table 2.2, and the magnetization curve of the motor is shown in figure 2.7.

H.P : 15 ; VOLTS : 400 ; FREQUENCY : 50 ∿/SEC. ; PHASES : 3;
POLES : 6 ; SLIPRING MOTOR
PRIMARY TO SECONDARY TRANSFORMATION RATIO 2.9

$$\left.\begin{array}{ll} R_1 = & \cdot 152\ \Omega \\ X_1 = & \cdot 56\ \Omega \\ R_2 = & \cdot 27\ \Omega \\ X_2 = & \cdot 56\ \Omega \\ X_{mu} = & 11\ \Omega \end{array}\right\}$$

ALL THE QUANTITIES ARE REFERRED TO THE SECONDARY.

RATED CURRENT = 12 AMPS. ; FULL LOAD TORQUE = 11·2 SYNCHRONOUS K·W.

TABLE 2.2

DETAILS OF THE MOTOR, THE CHARACTERISTICS OF WHICH ARE SHOWN IN FIGS.

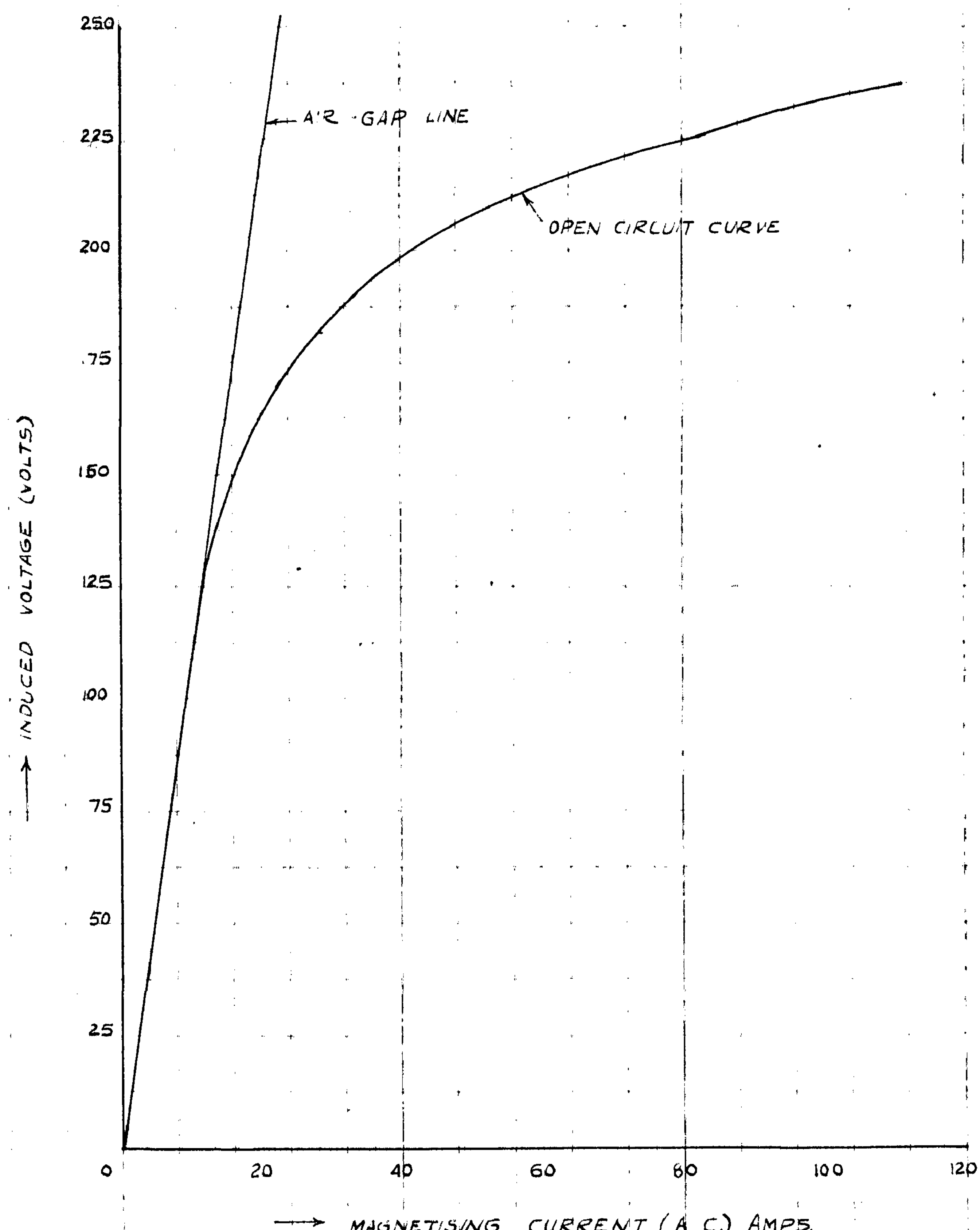

FIG. 2·7

OPEN CIRCUIT CHARACTERISTIC OF THE INDUCTION MOTOR
(DETAILS OF WHCH ARE GIVEN IN TABLE 2.2)

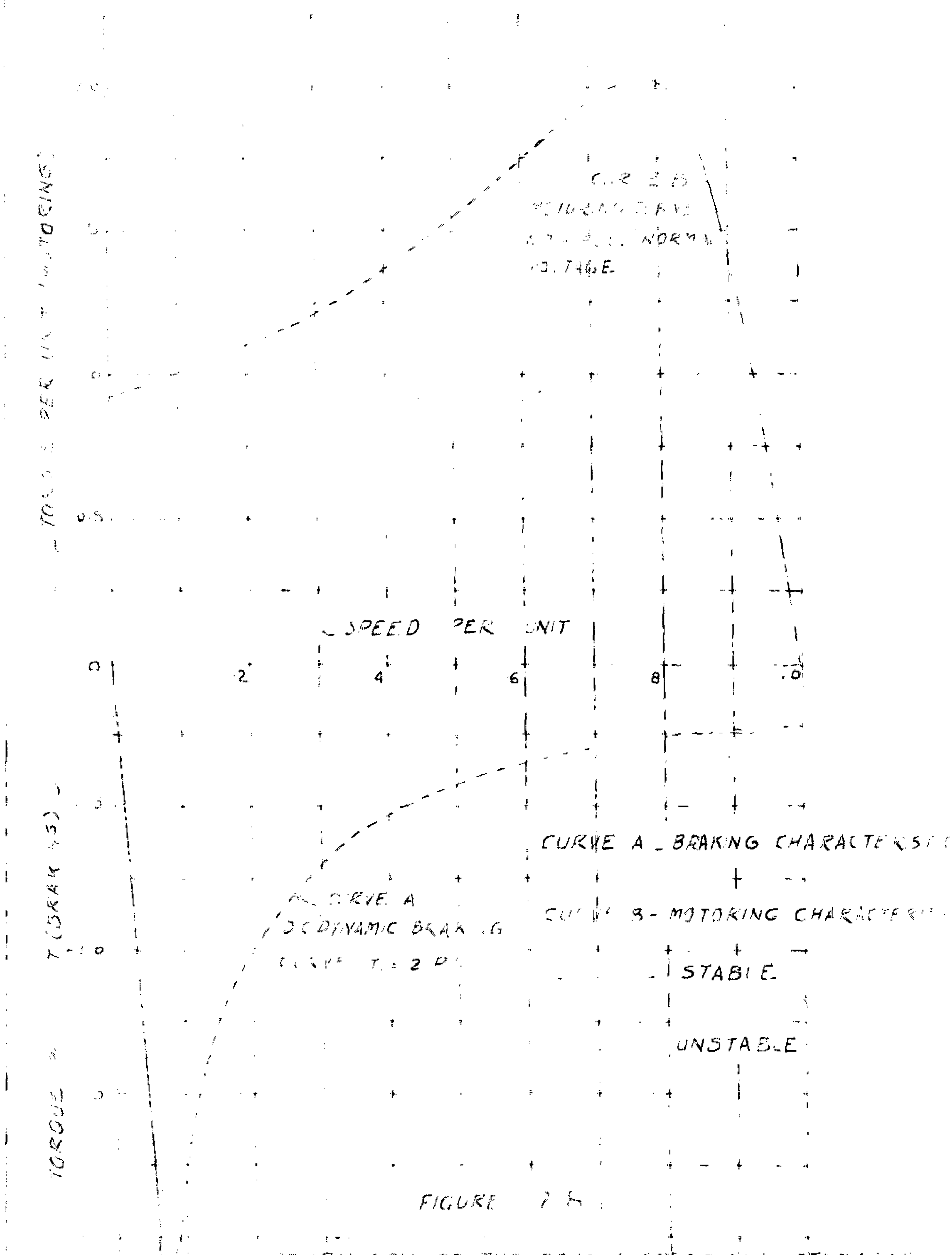

FIGURE 7.5

COMPARISON OF THE TORQUE SPEED CHARACTERISTICS OF AN INDUCTION MOTOR [illegible] DYNAMIC BRAKING [illegible]

The braking curve shown has been obtained for a stator excitation current equal to twice the rated current of the motor. It can be noticed that there is a striking similarity between the braking and motoring curves, the reason for which has been mentioned in article 2.1. But this similarity cannot be carried too far for a direct comparison because of the entirely different conditions under which the curves are obtained. But at least the curves indicate a reversal in the operation.

Both the curves have stable and unstable regions of operation, the dotted portions showing unstable operation, and the thick lines showing the stable regions. Also there is an optimum braking torqu at some value of the ratio of Resistance R_2 and the speed, in both the cases.

Taking the braking characteristic into consideration, it can be seen that any decrease in speed in the dotted portion of the curve, results in an increase in the braking torque and the machine decelerates further, giving an unstable operation. This unstable region continues upto the maximum torque point after which the performance is stable. Any decrease in speed in the stable region is followed by a decreased torque, and the torque reduces to zero at standstill. Thus, the speed at which the maximum torque occurs can be termed as critical braking speed[22] for the particular value of the secondary resistance R_2. The shape of the braking curve is evidently not satisfactory giving only a very low torque at higher speeds. Also at speeds close to standstill very low torque values are obtained.

As discussed in article 2.8 the same torque/speed curve A can be used for any other value of rotor resistance R_3 by multiplying the speed scale by $\frac{R_3}{R_2}$ where R_2 is the former value of the rotor resistance. Evidently the speed at which the maximum torque occurs is proportionately increased with an increase in the value of the secondary resistance. Thus the behaviour of the characteristic with the secondary resistance at once suggests that better effective braking is obtained in case of slip-ring induction motors, by suitably decreasing the value of R_2 from a top value at top speed to lower values at lower speeds. But as the speed/torque characteristic is unstable beyond the maximum torque value, with a pronounced steepness of the curve in that region, an attempt to effect a proportional decrease in resistance with decreasing speeds to get the maximum braking torque at all speeds, can result in unstable operation and subsequent loss of control in case of an overhauling load unless properly manoevered. Hence the incorporation of this principle depends on a closed loop control system being adopted in such cases.

In practice the maximum torque obtainable with an exciting current equivalent to the rated current is insufficient to meet the braking duty in many applications, even after suitable adjustment of the rotor resistance in the required speed range. Hence the only other alternative is to increase the exciting current I_1 to higher values.

A set of torque/speed characteristics compiled from test results published by Harrison[20] and Butler[22] for different values of the stator exciting current are shown in fig. 2.9.

Curve A is the torque/speed characteristic with an exciting current I_1 equal to the rated motor current. It can be clearly seen that that the maximum braking torque for this curve is only about 80% of the rated full load torque of the machine which seldom

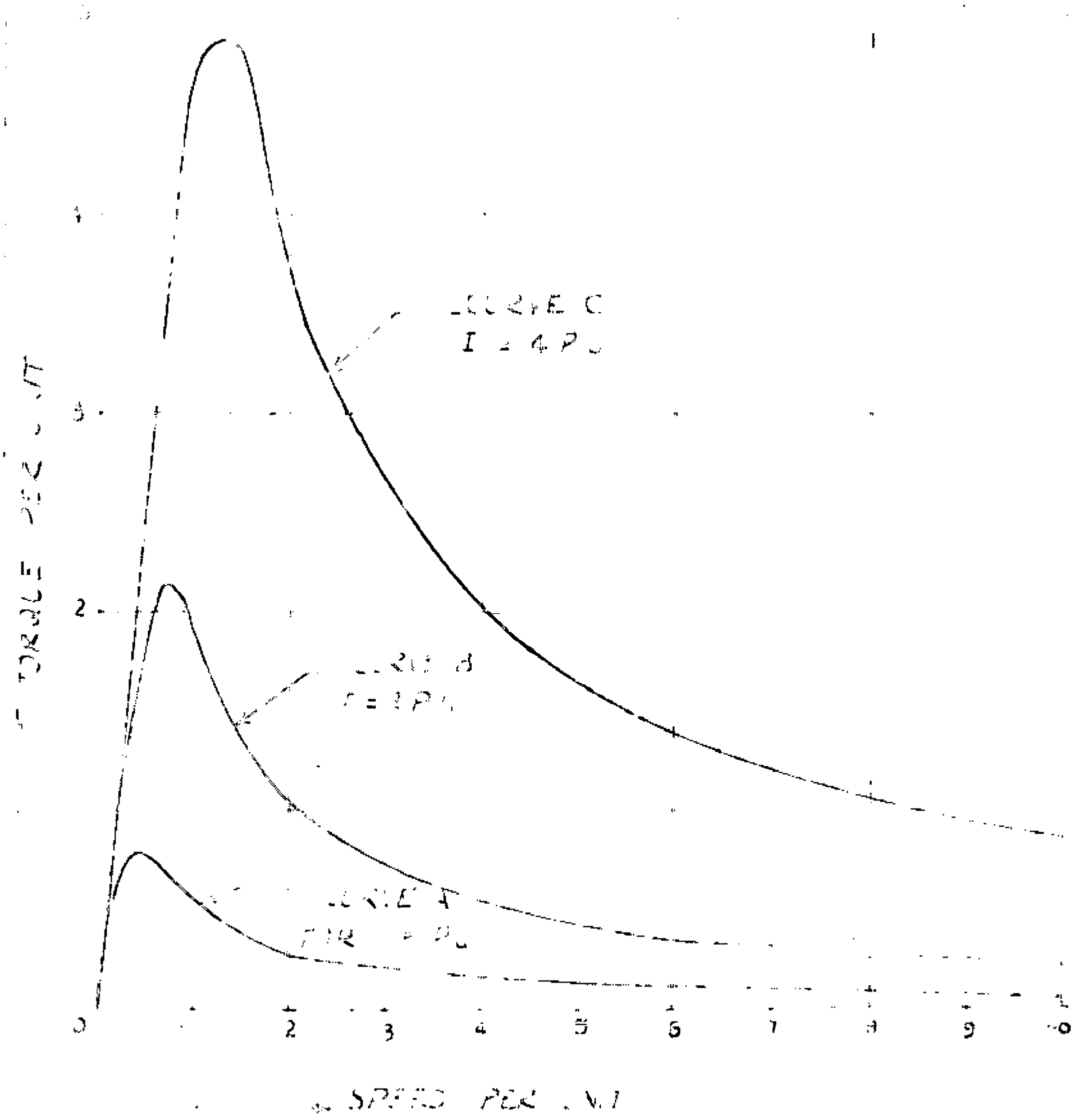

FIG 2·9

[illegible] CHARACTERISTICS OF AN [illegible] MOTOR [illegible]
[illegible] DYNAMIC BRAKING (MOTOR DETAILS ARE GIVEN IN TABLE [illegible]

satisfies the braking requirements in practice. The torque at higher values of the speed is pretty low amounting hardly to 10% of the rated torque which definitely cannot give any satisfactory performance. Curves B and C are the characteristics when the exciting currents are twice and four times the value of the rated current respectively.

From equation 2.7 it is clear that the torque is directly proportional to the square of the exciting current I_1 if there were no saturation. It is clear from Fig. 2.9 that such a proportionate increase in torque is not obtained in the regions of the maximum torque and all through the stable portions of the characteristics. Also it can be noticed that, as the excitation is increased the maximum torque occurs at a higher value of the speed, for the same value of rotor resistance. Hence there is an increase in the critical braking speed due to the effect of saturation.

In order to have a clearer conception of the effect of saturation on the torque/speed characteristics, the figure 2.10 is drawn[22]. The ideal characteristic shown in the figure 2.10 is that obtained for the condition of no magnetic saturation with an excitation current equal to rated current of the motor. Curve A shows the actual torque/speed characteristic with an excitation equal to rated current, and the torque values are expressed in per unit of the ideal maximum value.

The curves B and C are for values of excitation twice and four times the rated current respectively, and the torque values for these curves are expressed in per unit of the corresponding ideal maximum values. Thus the actual torque scale for curves B and C will be four times and 16 times the scale shown in the figure. The regions in which the corresponding curves are coincident with the

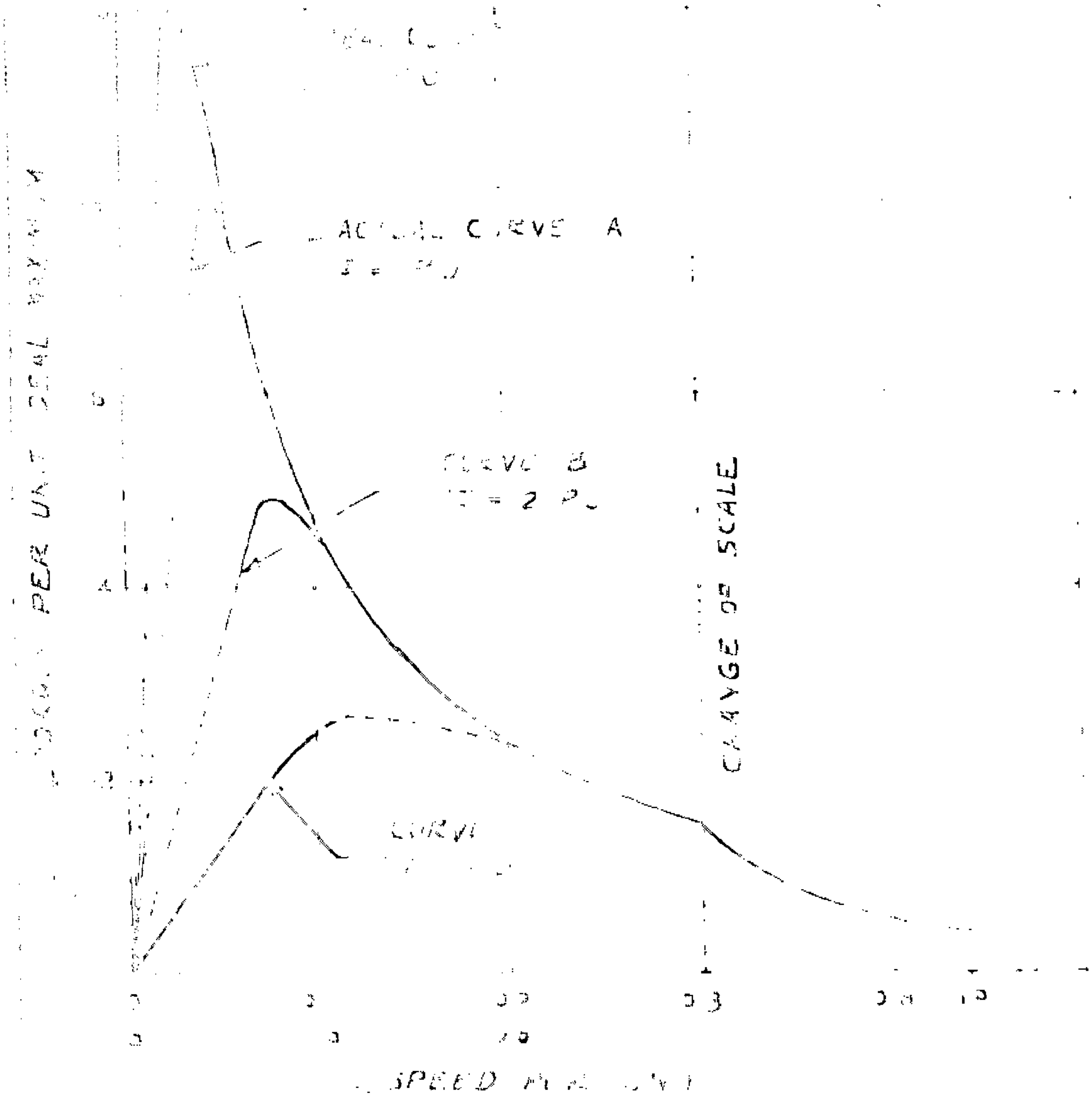

FIG 2. [illegible]

TORQUE-SPEED CHACACTERISTICS OF AN INDUCTON MOTOR UNDERGOING D.C. DYNAMIC BRAKING (MOTOR DETAILS ARE GIVEN IN TABLE [illegible] ideal characteristic shown in the figure, indicates that saturation is absent in those regions for that particular value of rotor resistance. Thus saturation sets in at 20% of the speed for curve C, at 10% for curve B and 6% for curve A, for $R_2 = .27\,\Omega$. When the resistance R_2 is increased the region of saturation effect will proportionately increase. Also it is evident that saturation distorts the stable portions of the characteristics severely, which is increasingly pronounced with higher values of excitation.

2.9.2. The nature of the torque/resistance characteristics.

The torque/resistance characteristics[22] obtained for a particular value of speed and three different values of the stator exciting current are shown in fig. 2.11. These curves are, for the same machine mentioned for obtaining the torque/speed curves.

As explained in article 2.8 the same curves can be used to represent the torque/resistance characteristics of the machine for a different value of speed N_3, by multiplying the resistance scale by $\frac{N_3}{N_2}$ where N_2 is the previous value of the speed. In fig. 2.11 the bottom scale for the resistance is for the characteristic at synchronous speed and the top scale is for a speed $\frac{1}{10}$ the synchronous speed.

The curves A, B, C are for the values of the excitation current, equal to one, two and four times the normal rated current of the motor. Starting from a high value of the rotor resistance when the resistance is decreased, the value of the torque increases for the particular value of speed showing stable operation. This action continues until the resistance at which the maximum torque occurs. Beyond this point a decrease in resistance results in a

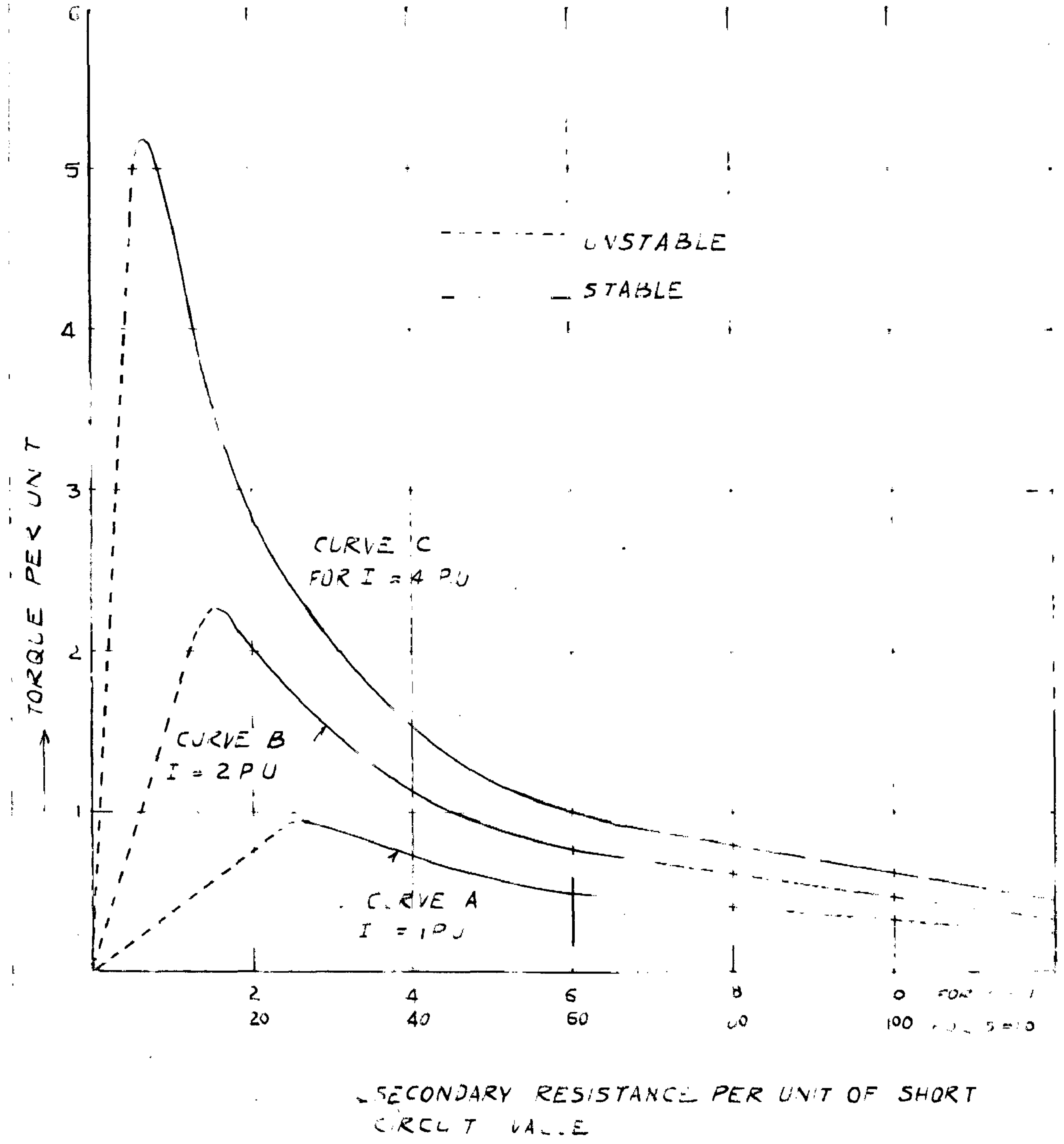

FIG 2.11

TORQUE-RESISTANCE CHARACTERISTICS OF AN INDUCTION MOTOR UNDER D C DYNAMIC BRAKING (MOTOR DETAILS GIVEN IN TABLE)

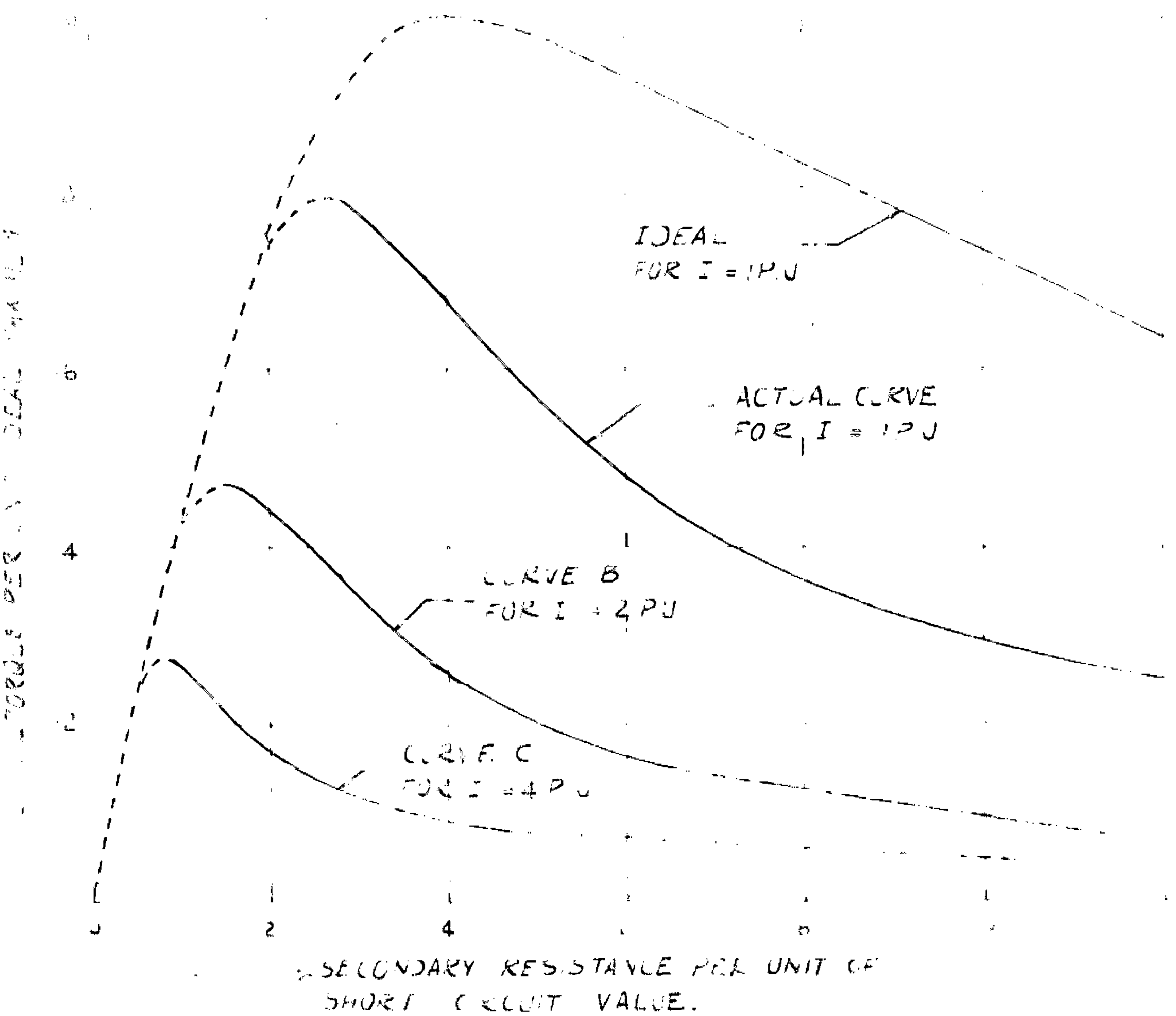

FIG 2.7

TORQUE RESISTANCE CHARACTERISTIC OF AN INDUCTION MOTOR UNDER D.C DYNAMIC BRAKING CODITIONS. (MOTOR DETAILS GIVEN IN TABLE decreased torque and consequent instability in the braking operation. The value of the resistance at which the maximum torque occurs can be termed as the critical braking resistance[22] for the particular value of speed.

In order to more clearly conceive the effect of saturation on the torque resistance characteristic, curves are drawn[22] as shown in figure 2.12. The ideal curve shown in the figure is that obtained for the hypothetical condition of no magnetic saturation with an excitation current equal to the rated current of the motor. Also the curve A is the actual characteristic with I_1 equal to the rated current. The curves B and C are for values of the excitation current equal to twice and four times the rated current respectively and it should be noted that the torque values for these curves are expressed in per unit values of the corresponding ideal curves. It is evident from fig. 2.12 that there is a pronounced effect of saturation on the stable portion of the characteristics. Also it can be noticed that there is a decrease in the critical resistance value with an increased excitation due to the effect of saturation.

Referring to figure 2.9 and 2.11 it can be seen that the shapes of the torque/speed and torque/resistance characteristics are not identical. In fact equation 2.8 shows that the torque/speed characteristic can be made to represent the torque/resistance curves, by multiplying the per unit speed scale by the value ($X_2 + X_m$) ohms., in the absence of saturation. Thus, saturation makes this impossible.

2.9.3. Summary of the nature of braking characteristics.

1. For normal values of rotor resistance low torques are obtained at higher speeds and very low torques at values

of speed close to standstill.

2. By varying the resistance (R_2) more effective braking torque can be obtained in a wider speed range.

3. An increase in torque all over the speed range can be obtained by increasing the exciting current well above the rated value for normal applications subject to the restriction of thermal capacity.

In practice a variation of the exciting current is automatically effected, depending on the rotor current, so that a continuous injection of a high current is avoided, by incorporating a closed loop control system for important applications such as mine winders.

2.10. Stopping Time.

The knowledge of the running down time from a higher speed to lower values or standstill under braking is primarily necessary for the selection of the braking scheme.

The torque obtained by equation 2.7 is only the braking torque produced electrically in the machine by the dynamic braking scheme. There are the other torques which have not been considered, which contribute towards deceleration such as those produced by windage, friction, iron and stray losses and the losses due to space-harmonics m.m.f.'s etc. If the dynamic braking torque as calculated from equation 2.7 is T_b at a particular speed and the loss torques which are not included in T_b is taken as T_L, at the same speed, then the total torque T_T producing deceleration is given by

$T_T = T_b + T_L$ at a particular speed, all the torque values being expressed in synchronous watts. Now the kinetic energy of a rotating mass is given by

$$K.E. = \tfrac{1}{2} J \omega^2 \text{ ft. lbs.}$$

where J is the moment of inertia expressed in lbs.ft.^{2} and ω is the angular velocity of the drive in radians/second.

Torque will be equal to rate of change of kinetic energy.

$$T_{lbs.ft.} = \frac{J}{32} \frac{d\omega}{dt} = \frac{J}{32.2} \times \frac{2\pi}{60} \times \frac{dN}{dt}$$

where torque is in lbs. feet and N is the speed in r.p.m.

$\therefore$ Torque is synchronous watts will be given by

$$T = \frac{2 N_s \pi}{60} \times \frac{J}{32.2} \times \frac{2\pi}{60} \times \frac{dN}{dt} \times \frac{550}{746}$$

$$= .000462 \ N_s J \frac{dN}{dt}$$

$$= K N_s \frac{dN}{dt}$$

where $K = .000462 J = 2 \times$kinetic energy in joules per r.p.m.^{2}

Hence for deceleration

$$T = - K N_s \frac{dN}{dt} \qquad 2.11$$

If $t = t_1$ at $N = n_1$ and $t = t_2$ at $N = n_2$

then

$$\int_{t_1}^{t_2} dt = - K N_s \int_{n_1}^{n_2} \frac{dN}{T} \qquad 2.12$$

and hence the time to decelerate from n_1 and n_2 is

$$t_2 - t_1 = K\ N_s \int_{n_2}^{n_1} \frac{dN}{T} \qquad .2.13$$

Unless n_2 is taken as a small quantity instead of zero an analytical solution of the above equation is not possible.

The right hand side of the equation is equal to the area under the curve $\frac{KN_s}{T}$ plotted against N as absissa between speeds n_1 and n_2, where T is the total torque $T_L + T_b$. Usually T_L versus speed characteristic is a straight line, and T_L is directly proportional to speed and can be determined experimentally. Once we know the relationship between T_L and N, this can be superimposed on the dynamic braking torque/speed characteristic to get the curve T_T versus speed. From this curve $\frac{1}{T_T}$ versus speed can be drawn. The area of this curve between n_1 and n_2 multiplied by the constant KN_s for that particular drive will give the value of time to decelerate from n_1 to n_2.

The method described above is rather tedious. But this has to be resorted to, in case an accurate prediction of the time for deceleration is necessary as in the case of automatic mine winders.

Alternatively in many applications, the loss torque is a small percentage of the total braking torque especially when the motor is driving a load of large moment of inertia. In such cases T_L can be neglected. Also in order to facilitate a mathematical solution to be obtained the dynamic braking torque/speed characteristic can be represented by two discontinuous curves. This has been evolved by Butler[24] and is given below.

Referring to fig. 2.13, OBD is the true torque/speed characteristic calculated using equations 2.1 to 2.7 for particular values of I_1, R_1 and X_2.

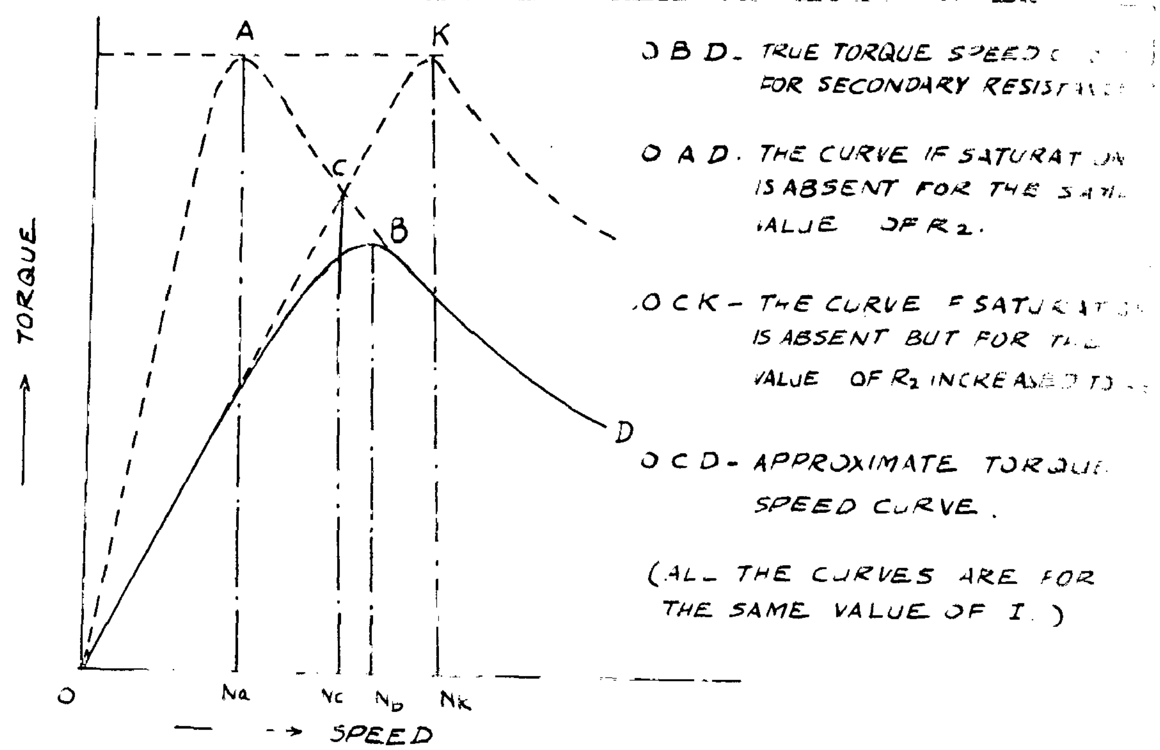

FIG. 2·13

FIGURE SHOWING THE APPROXIMATION OF TORQUE-SPEED CHARACTERISTIC UNDER D.C. DYNAMIC BRAKING OF AN INDUCTION MOTOR.

Suppose X_m is assumed to be constant at its unsaturated value X_{mu}, curve OACD will be obtained for the same value of I_1, R_2 and X_2 . Curve OCK can be drawn again keeping X_m at its unsaturated value X_{mu}, but increasing R_2 to R_3 (keeping I_1 and X_2 same) such that

$$R_3 = p\, R_2 \qquad 2.14$$

where $p = \dfrac{X_{mu}}{X_{ms}}$, X_{ms} being the saturated value of the magnetizing reactance obtained from the open circuit characteristic of the machine corresponding to a current of I_1. C is the point of intersection of curves OCK and OACD.

It can be shown that the two discontinuous curves OC and CD together can approximately represent OBD, for the purpose of the calculation of the running down time.

We know that the saturation affects the performance at low values of speed due to reduced opposition of the secondary current to the primary flux, and for normal values of rotor resistance saturation is virtually absent at higher values of speed. Hence, the portion CD of the curve OACD, calculated based on the assumption of no magnetic saturation can approximately represent BD. Now at speeds close to standstill $(X_m + X_2)$ is small compared to $\left(\frac{R_2}{S}\right)$ and hence equation 2.7 can be re-written as below keeping in mind that at these low speeds $X_m = X_{ms}$.

$$\therefore T = m. \frac{I_1^2 X_{ms}^2 S}{R_2}$$

Therefore the initial slope of the curve OMD is

$$\left(\frac{dT}{dN}\right)_{N=0} = N_s\left(\frac{dT}{dS}\right)_{S=0}$$

$$= m. \frac{I_1^2 X_{ms}^2}{R_2} N_s$$

As far as the curve OCK is concerned $X_m = X_{mu}$ and the secondary resistance is pR_2. Hence the initial slope of curve OCK will be

$$N_s\left(\frac{dT}{dS}\right)_{S=0} = \frac{m I_1^2 X_{mu}^2 N_s}{pR_2}$$

$$= \frac{m I_1^2 X_{ms}^2 N_s}{R_2} \quad \text{because } p = \frac{X_{mu}}{X_{ms}}$$

Thus the initial slopes of the curves OCK and OBD are the same. The portion OC can be approximately taken to represent OD.

Hence, the curves OC and CD approximately represent OBD. It can be noticed that the area of the portion between the curve OCD and OBD is not going to affect the value of the stopping time appreciably because it is the unstable portion BD, that essentially contributes most to the stopping time for the normal values of R_2. This approximation will give slightly lower value of stopping time because the area under OCD is greater than that under OBD; but after all the loss torques have been neglected and errors tend to cancel rather than being cumulative. Also it may be noted that there is a sharp cut off, of speed when the speed has reached below about 1/10th of the synchronous speed due to the presence of locking torque[24] arising from minimum magnetic reluctance positions of the rotor with respect to the stator. It may be noticed that in order to facilitate to evolve the solution of equation 2.13 a small value of the speed n_2 has to be chosen instead of zero. In the light of the loss torques having been neglected this can also be justified to a certain extent.

Now suppose T_a is the maximum value of torque for curves OAD and OCK from equation 2.9.We get

$$T_a = m. \frac{I_1^2 \quad X_{mu}^2}{2(X_2 + X_{mu})} \qquad 2.9a$$

The equation for the curve OAD can be written from equations 2.7 and 2.9a which gives

$$T = \frac{2\ T_a\ SS_k}{S_K^2 + S^2} = \frac{2\ T_a\ NN_k}{N_k^2 + N^2} \qquad 2.14$$

where S_k is the value of the fractional slip at the point K in fig. 2.13 and N_k is value of speed at the point K.

Similarly the equation for curve OCK is given by

$$T = \frac{2T_a \; S \; S_a}{S_a^2 + S^2} = \frac{2T_a \; N \; N_a}{N_a^2 + N^2} \qquad 2.15$$

where Na and Sa are the values of the speed and the fractional speed at point A in Fig. 2.13.

From equations 2.14 and 2.15 the point of intersection C can be obtained giving

$$N_c = N_a \sqrt{p} \qquad 2.16$$

$$T_c = \frac{2 \; T_a}{\sqrt{p} + \frac{1}{\sqrt{p}}} \qquad 2.17$$

Thus equations 2.14 to 2.17 define the curve OCK.

Hence the time taken to decelerate from a speed n_1 to speed n_2 can be obtained from equations 2.13 to 2.17.

$$t = t_2 - t_1 = \frac{KN_s}{2 \; T_a} \int_{N_c}^{n_1} \frac{N_a^2 + N^2}{NN_a} \, dN + \frac{KN_s}{2T_a} \int_{n_2}^{N_c} \frac{N_k^2 + N^2}{NN_k} \, dN$$

$$= \frac{KN_s}{2T_a} \left[\frac{N_c^2 - n_2^2}{2 \; N_k} + N_k \log \frac{N_c}{n_2} + \frac{n_1^2 - N_c^2}{2 \; N_a} + N_a \log \frac{n_1}{N_c} \right] \qquad 2.18$$

The minimum stopping time from synchronous speed N_s to a speed n_2, for a fixed value of R_2 will occur when $\frac{dt}{dN_c} = 0$ and can be shown to be

$$t_{min.} = \frac{KN_s^3}{2T_a \; N_a} \left[1 - \frac{n_2^2}{pN_s^2} - (p - 1) \frac{N_a^2}{N_s^2} \right] \qquad 2.19a$$

This occurs when N_a satisfies the following equation

$$1 - \frac{n_2^2}{p\ N_s^2} = \frac{N_a^2}{N_s^2} (p - 1) \left(1+2 \log \frac{N_c}{N_s}\right) - 2 \frac{N_c^2}{N_s^2} \log \frac{n_2}{N_s} \qquad 2.19b$$

Thus for a particular value of I_1 and X_2 the minimum stopping time will occur if R_2 is adjusted to the value defined by equation 2.19 b. This is the optimum value of fixed rotor resistance for a particular value of excitation I_1.

Ideal Minimum stopping time.

If in case of a slip-ring motor R_2 is continuously adjusted to maintain the braking torque at its maximum value T_b given by curve OBD, throughout the speed range, then we get the ideal minimum stopping time which can be straightaway obtained from equation 2.13 as

$$t_{i.m.} = KN_s \int_0^{N_s} \frac{dN}{T_b} = \frac{KN_s^2}{T_b} \qquad 2.20$$

After calculating $t_{i.m.}$ it can be found out as to how much less time is obtained by this control arrangement, than the time obtained by keeping R_2 as constant at its optimum value defined by equation 2.19 b. This is a significant clue in deciding whether the initial and maintenance cost of the control arrangement is worthwhile for the sake of the reduction in the stopping time. Experimental results[24] show that usually only a reduction of about 25% is attained in practice.

If magnetic saturation were absent the ideal minimum stopping time would have been $\frac{K\ N_s^2}{T_a}$ and thus we can see that the stopping time $t_{i.m.}$ would have been reduced to $\frac{T_b}{T_a}$ times, and hence the energy losses in the primary circuit also could have been reduced by the same percentage.

The method described above for finding out the stopping time will evolve reasonably accurate results and can be used in applications where such accuracy is warranted.

But there are many small applications in which a desired stopping time is mentioned and the corresponding value of the direct current excitation has to be found out. In their paper, Harrel and Hough[4] have given empirical curves showing the relationship between d.c. watts per pound of effective braking torque required versus the number of poles. They are based on a wide range of test results on squirrel-cage motors having the same physical frame size but wound for 4,8 and 12 poles each with 3 different rotor resistance. In many applications where squirrel cage motors below 10 h.p. are used it may be required to stop a particular load in a given time and in such cases these curves could be used to find the required d.c. value of stator current. But this entirely depends on whether the type of motor used is comparable in size with the motors tested by the authors. Thus, each manufacturer may have his own type of design and as such it is impossible to generalise this method. For example in America 60 ~/sec. is the industrial supply frequency and the motors tested are designed for normal operation at 60 ~/sec. whereas in many other countries like ours 50 ~/sec. is the standard frequency.

Bendz[7] has also given an empirical curve of D.C. amps on percentage of full load motor rating versus $\frac{\text{Average braking Torque}}{\text{Motor starting torque}}$

Knowing the motor starting torque and the stopping time allowed, and the moment of inertia of the load the direct current required to be injected can be evaluated using the curves given. The author[7] claim that this will give sufficiently good results for motors from $\frac{1}{4}$ to 10 h.p. As mentioned before such empirical curves have their sphere of restricted use.

2.11 Energy losses during braking.

The total energy losses during dynamic braking is the sum of the secondary circuit loss and the primary circuit loss.

In the secondary circuit the energy losses during an interval of time t_1 to t_2 seconds in joules is given by

$$W_2 = \int_{t_1}^{t_2} m \, I_2^2 \, R_2 \, dt \qquad 2.21$$

From equations 2.7 and 2.21 we get

$$W_2 = \int_{t_1}^{t_2} \frac{N}{N_s} \, T \, dt \qquad 2.22$$

Substituting equation 2.11 in 2.22 we get

$$W_2 = -K \int_{n_1}^{n_2} N dN = \frac{K (n_1^2 - n_2^2)}{2} \qquad 2.23$$

If $n_1 = N_s$ and $n_2 = 0$ we get

$$W_2 = \frac{KN_s^2}{2} = W_o \qquad 2.24$$

= kinetic energy of rotating masses at speed N_s

Hence all the kinetic energy is dissipated as heat in the rotor circuit. Because of the effect of windage and friction losses, the actual value of W_0 will be slightly less. The losses in the primary circuit is given by

$$W_1 = m\, I_1^2\, R_1\, t \qquad 2.25$$

Equation 2.24 shows that theoretically the energy losses in the rotor circuit is independent of the magnitude of excitation applied, neglecting other losses. Evidently there is no flow of power from the rotor to the stator or vice-versa, and the stator field is just an agent in the transfer of power from the rotating masses to the rotor circuit.

The primary circuit energy losses evidently depends on the time for stopping the drive for a fixed value of excitation. The time taken is defined by the equation 2.18 substituting suitable limits for n_1 and n_2. Also it is evident that magnetic saturation will affect the total energy losses of the primary winding because the time to stop the drive would have been less if magnetic saturation were absent.

CHAPTER - 3

MACHINE PERFORMANCE UNDER D.C.DYNAMIC BRAKING CONDITIONS-HELLMOND'S ANALYSIS

3.1. Hellmond's analysis.

3.2. Comparison of Hellmond's analysis and the induction motor approach of analysis.

CHAPTER - 3

MACHINE PERFORMANCE UNDER DYNAMIC BRAKING CONDITIONS-HELLMOND'S ANALYSIS

3.1. Hellmond's Analysis[5]

Hellmond in his contribution to this field directly based his approach on fundamental flux considerations.

Considering a 3 phase induction motor with a balanced winding let it be assumed that the machine is running almost at synchronous speed when the a.c. supply is switched off and a suitable stable d.c. voltage is applied across two of the terminals of the stator winding.

Referring to figure 3.1, the rotor current I_2, will cause voltage drops $I_2 R_2 = E_R$ and $I_2 X_2 = E_x$, across the resistance and reactance of the rotor, the sum of these two being equal to the rotor induced e.m.f. E_2.

In order to induce an e.m.f. component E_R there should be a field ϕR leading the same by 90° and a field ϕ_X is required for inducing the component E_X. The resultant field ϕ_S required for inducing the voltage E_2, is the sum of ϕ_R and ϕ_X. From the magnetization curve, we can then find out the magnetizing current I_m required to establish a field ϕ_S. Hence the total excitation I_1 required at the particular speed N_s (as we have assumed that the machine is at speed N_s at this instant) is the sum of I_m and I_2. The conversion of the alternating current into equivalent direct current and vice-versa is explained in

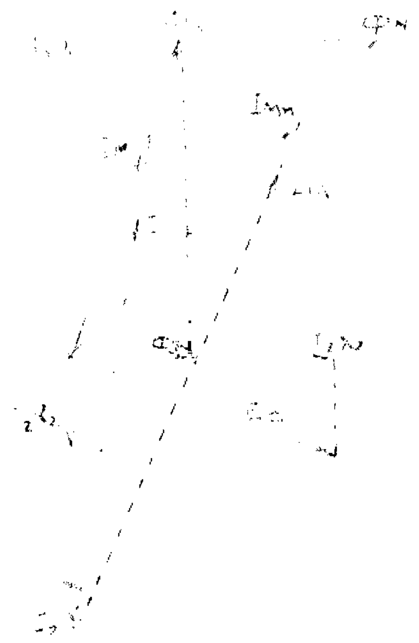

FIG 3.1

VECTOR DIAGRAM OF THE CURRENTS, VOLTAGES AND [illegible] DYNAMIC BRAKING OF AN INDUCTION MOTOR

article 2.2. As the machine is undergoing braking the speed decreases. At any other speed N ($N < N_s$) the value of E_R remains unchanged but the frequency of E_R has changed to $\frac{N}{N_s}$ times the original value, as the machine has decelerated to speed N. Hence in order to induce the same magnitude E_R , the flux should increase by the ratio $\frac{N_s}{N}$, so that the new value of field required will be

$$\phi_{RN} = \phi_R \times \frac{N_s}{N}$$

Considering the reactance drop E_x, the frequency of E_x has changed to $\frac{N}{N_s}$ times its original value. But for the same current I_2, the magnitude of E_x at the speed N has also changed to $E_x \frac{N}{N_s} = E_{xN}$, because the reactance will change proportional to the frequency. Hence the flux required to induce the e.m.f. E_{xN} remains the same because both the magnitude of the e.m.f. and its frequency have changed in the same proportion. Thus ϕ_x remains the same at all speeds. The resultant of ϕ_{RN} and ϕ_x will now give ϕ_N and from the magnetization curve I_{Mn} and hence the excitation I_{1n} can be found out as before.

Thus for a particular value of I_2 and at various values of the speed N, a set of calculations are made to get the corresponding values of I_1 and a graph I_1 versus speed is plotted. Similarly for various other assumed values of I_2, graphs are obtained showing the relationship between I_1 and N. From this set of curves, values of the speed and the rotor current are obtained for a particular desired value of I_1.

The braking torque in synchronous watts at a particular speed N is evidently equal to the power dissipated in the rotor circuit i.e. $m E_{RN} I_2 = m I_2^2 R_2 \left(\frac{N_s}{N} \right)$ from which the torque/speed characteristics are evolved for a particular value of I_1.

3.2. Hellmond's analysis and Induction Motor approach of Analysis - a comparison.

It can be readily seen that Hellmond's method of analysis will lead to exactly identical results as that obtained by the induction motor approach as described in Chapter 2. The difference lies in the procedure adopted, which is not reduced to a mathematical form in the analysis by Hellmond, thereby involving tedious and cumbersome calculations of individual values. Thus even though the results will be identical by both the methods, practical utility of Hellmond's method is rather limited. It is worthwhile pointing out that the method has been described in this dissertation only from the point of view of academic interest because Hellmond's method is the oldest analysis of the problem of dynamic braking of an induction motor by d.c. injection.

CHAPTER -4

MACHINE PERFORMANCE UNDER D.C. DYNAMIC BRAKING CONDITIONS — THE SYNCHRONOUS IMPEDENCE METHOD OF ANALYSIS

4.1. Viewing the induction motor under d.c. braking as an alternator.

4.2. The synchronous impedence method as adopted to d.c. braking of induction motors.

CHAPTER - 4

MACHINE PERFORMANCE UNDER BRAKING CONDITIONS THE SYNCHRONOUS IMPEDENCE METHOD[13] OF ANALYSIS

4.1. Viewing the induction motor under d.c.braking as an alternator

The induction motor undergoing d.c. dynamic braking can be viewed as an alternator with a continuously varying speed. The stator winding in which the direct current is injected, establishes a magnetic field in space which is comparable to that produced by the field winding of a cylindrical rotor alternator. The rotor of the induction motor under dynamic braking conditions is analogous to the armature of an alternator. In the case of squirrel-cage motors the rotor winding is invariably short-circuited and therefore it is similar to a short-circuited armature of an alternator. In the case of slip ring motors there is the provision for introducing external secondary resistances which are equivalent to the load resistances of an alternator. Also, whereas in a normal alternator the speed is kept constant, the induction motor under d.c. braking is having the speed continuously varied from almost the synchronous speed to zero, though in cases where overhauling loads are present as in the case of crane hoists etc., the machine may be operated at constant value of speed under braking conditions subject to stable operation. Thus the methods of calculating the alternator performance can also be suitably adopted to effect an analysis of the braking characteristics of an induction motor. In this chapter the synchronous impedence method as applied to the dynamic braking of an induction motor is described.

4.2. The Synchronous impedence method as adopted to the d.c. braking of induction motors.

LaPierre and Metaxas[13] have adopted the synchronous impedence method with slight modifications for calculating the braking characteristics of a squirrel-cage induction motor, the method being equally applicable to slip-ring motors as well.

The effect of the reaction of the rotor current I_2 on the rotor induced voltage is exactly similar to that of the leakage reactance drop of the rotor winding, and they act in the same direction. At a particular speed, the voltage drop produced by the rotor leakage reactance is proportional to the rotor current I_2 . Similarly if saturation is absent the effect of the rotor m.m.f. on the voltage induced is also proportional to the rotor current at the same speed. For a particular value of rotor current, both of these effects vary in the same proportion, and are directly proportional to the speed. Because of the similarity in effects that they produce they can be combined and expressed in terms of a total reactance X_s, known as synchronous reactance which is made up of the leakage reactance X_2 and a fictitious reactance X_m. The fictitious reactance X_m, then causes a voltage drop with a current I_2 which is that produced by the effect of the rotor current on the stator flux. It may be noted that all the quantities X_s, X_m and X_2 are referred to the same angular frequency ω_S. Evidently when saturation is present X_s will vary. In the synchronous impedence method X_s is assumed to be a constant at a compromised value.

The synchronous impedence Z_s is the total impedence of the closed rotor circuit which is made up of the effective resistance R_2 and the synchronous reactance X_s which gives

$$Z_s = R_2 + jX_s \qquad 4.1$$

For a particular value of the stator current I_D, the equivalent alternating current I_1 is determined depending on the type of connection as described in article 2.2. Corresponding to this value of the exciting current the open circuit voltage E_2, of the rotor is determined from the open circuit characteristic at the synchronous speed. It should be noted that E_2 is the value of rotor induced e.m.f, if the effect of the rotor current on the stator flux is not present for that particular value of excitation. At any other speed N_2, the open circuit voltage for the same value of exciting current is equal to $E_2 \frac{N_2}{N_s}$. Also the synchronous impedence of the closed rotor circuit at any speed N_2 will be given by

$$(Z_s)_{N2} = R_2 + \left(\frac{N2}{N_s}\right) X_s \qquad 4.2$$

Hence the rotor current at any speed N_2 will be given by

$$I_2 = \frac{E_2 \frac{N_2}{N_s}}{\sqrt{R_2^2 + X_s^2 \left(\frac{N_2}{N_s}\right)^2}} = \frac{E_2 S}{\sqrt{R_2^2 + S^2 X_s^2}}$$

$$= \frac{C N_2}{\sqrt{R_2^2 + P N_2^2}} \qquad 4.3$$

where $C = \frac{E2}{N_s}$ = Induced voltage per r.p.m. for a particular value of excitation I_1, and $P = \frac{X_s}{N_s}$ = the synchronous reactance per r.p.m.

The torque is synchronous watts

$$T = m I_2^2 R_2 \frac{N_s}{N_2} = \frac{m E_2^2 \frac{R_2}{S}}{\left(\frac{R_2}{S}\right)^2 + X_s^2}$$

$$= m \cdot \frac{C^2 N_2 N_s}{R_2^2 + PN_2^2} \qquad 4.4$$

Determination of C and P

LaPierre and Metaxas[13] have suggested the following method to determine C and P.

The value of E_2 is obtained from the open circuit characteristic of the machine (Ref. article 2.4.3). This is the value of voltage obtained from the open circuit curve at a value of the current equal to the equivalent alternating current of the stator excitation. Knowing E_2, the value of C can be calculated.

The value of X_s is obtained from the open circuit and short circuit characteristics. As applied to synchronous machines we know that the short circuit characteristic is the relationship between the field current and the armature current, with the armature short-circuited and driven at synchronous speed. Under these conditions the armature m.m.f. strongly reacts with the field m.m.f. and the magnetic saturation of the machine will be absent. Hence the short circuit characteristic will be a straight line except at very high currents. When applied to an induction motor, the short circuit characteristic can be determined by applying a reduced 3 phase voltage at normal frequency to the stator with the rotor kept at standstill; and measuring the stator current. In case of slip-ring induction motors the rotor short circuit current can be measured. In case of squirrel-cage motors the rotor current is calculated using the equivalent circuit under standstill conditions, as shown in figure 4.1. The value of X_{mu} is readily obtained from the air gap line of the open circuit curve.

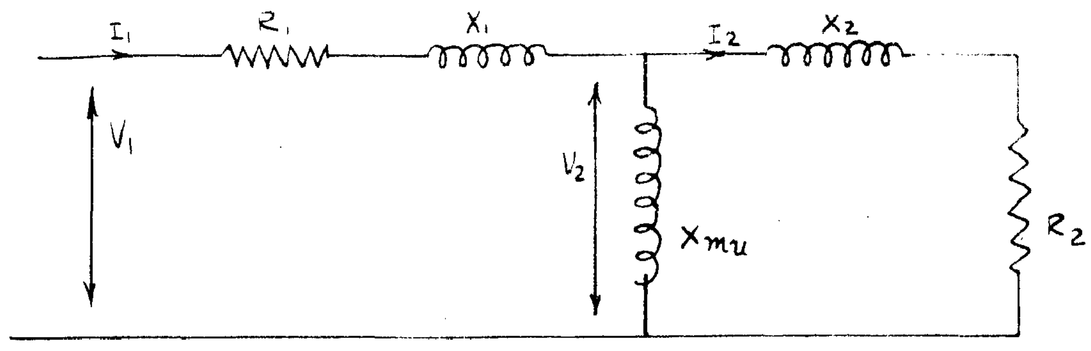

FIG. 4.1

EQUIVALENT CIRCUIT OF ONE PHASE OF AN INDUCTION MOTOR WITH THE ROTOR KEPT AT STANDSTILL

Then the short circuit characteristic is the relationship between the stator current along the X-axis and the rotor current referred to the stator along the Y-axis. Now at a value of the current, equal to the equivalent a.c.value of the direct current applied, the induced e.m.f. E_2 is obtained from the open circuit curve and the value of rotor current I_2 from the short-circuit line. The synchronous impedence is then equal to $\frac{E_2}{I_2}$ and can be taken as equal to the synchronous reactance X_s, because X_s is quite high as compared to R_2.

The resistance R_2 can be taken as a constant at the effective resistance value determined at normal frequency as explained in article 2.4. Alternatively a curve showing the relationship between the effective resistance and the frequency can be plotted which can be used for the performance calculations.

Having determined the values of the parameters the performance calculations can be carried out using equation 4.4 and the braking characteristics of the machine can be obtained.

CHAPTER - 5

DISCUSSION AND COMPARISON OF THE SYNCHRONOUS IMPEDENCE METHOD AND THE INDUCTION MOTOR APPROACH OF ANALYSIS

CHAPTER -5

DISCUSSION AND COMPARISON OF THE SYNCHRONOUS IMPEDENCE METHOD AND THE INDUCTION MOTOR APPROACH OF ANALYSIS

Before comparing the relative merits of the above two methods of analysis of an induction motor under d.c. dynamic braking, it is worthwhile pointing out, that basically analysing the problem either as an induction motor or as an alternator should give identical results. It is the adaptation of the parameters to suit the changed conditions of operation that decides the validity of the results. As a matter of fact, the analysis of the problem by Hellmond[5] being from fundamental flux considerations naturally incorporates both the alternator and induction motor theories in it.

Comparing equations 2.7 and 4.4, we can evidently conclude that they will be exactly identical provided the following relationships are satisfied.

$$X_2 + X_m = X_s \qquad \text{(a)}$$

$$I_1 \; X_m = E_2 \qquad \text{(b)}$$

By the very definitions of the parameters both the above conditions are satisfied, if saturation is absent with a value of magnetizing current equal to the exciting current I_1. Thus both the synchronous impedence method and the induction motor method will give identical results under unsaturated conditions.

But under saturated conditions of operation the proposition becomes very different. When magnetic saturation is present X_m is a variable according to the induction motor method, whereas as per the synchronous impedence method both E_2 and X_s are kept as constant values for a particular value of excitation. Thus under saturated conditions, the relations a and b cannot be satisfied individually.

In order to effect a better comparison of the equations under conditions of magnetic saturation we can modify the presentation of equation 4.4 as follows. For a value of I_1 from the open circuit characteristic let the value of the magnetizing reactance be X_{ms}. Then

$$E_2 = I_1 X_{ms} \qquad 5.1$$

Also by definition if there is no saturation the value of unsaturated synchronous reactance will be given by

$$X_{su} = X_{mu} + X_2 \qquad 6.2$$

Under saturated conditions, a compromised value of X_s has been arrived at, from the open circuit and short circuit characteristics of the machine. Under short circuit conditions obtained by blocking the rotor at standstill and applying a reduced 3 phase voltage, unsaturated operating conditions prevail and hence neglecting the resistance R_2 , the ratio of the rotor current (referred to stator) to the stator current will be almost equal to $\frac{X_{mu}}{X_{mu} + X_2}$ (Refer figure 4.1). Hence the short circuit characteristic as applied to an induction motor has a slope of

$$m = \mathrm{Tan}^{-1} \frac{X_{mu}}{X_{mu} + X_2} \qquad 5.3$$

and the minimum value of X_m for the particular excitation I_1 will be X_{ms}. Hence the first term of the denominator of equation 5.6 will be always less than the corresponding term in equation 5.5. Also the latter term of the denominator of equation 5.6 will be always greater than the corresponding term in equation 5.5 When $X_2 = 0$, as compared to the synchronous impedence method, the induction motor method will always give greater values of torque all through the speed range. Also in the region of the speed where saturation is absent, torque values as obtained from equation 5.6 will be greater than those obtained from the equation 5.5.We can also expect that for normal values of X_2, the synchronous impedence method will give lesser torque values all through the speed range.

It can be shown from equation 5.5 that the maximum value of the torque is obtained when

$$\frac{R_2}{S} = \frac{X_{ms}}{X_{mu}} (X_{mu} + X_2) \qquad 5.6$$

The value of the maximum torque will be

$$T_{max} = I_1^2 \frac{X_{mu} \quad X_{ms}}{2 (X_{mu} + X_2)} \qquad 5.7$$

Comparing equations 2.9 and 5.7 and keeping in mind that X_{ms} can be as low as $\frac{X_{mu}}{5}$ or $\frac{X_{mu}}{6}$ for usual values of excitation, we can conclude that the maximum torque values estimated by the synchronous impedence method will be very

It is interesting to note that the short circuit characteristic proposed to be obtained by a test by LaPierre and Metaxas seems unwarranted in the light of the equation 5.3.

Now the value of X_s used in equation 4.4, for the particular value of I_1 will be

$$X_s = \frac{E_2}{(I_2) \text{ short circuit}} = \frac{E_2}{I_1 \cdot \frac{X_{mu}}{X_{mu} + X_2}}$$

$$= \frac{X_{ms}}{X_{mu}} (X_{mu} + X_2) \qquad 5.4$$

It can be seen that equation 5.4 reduces to equation 5.2 when $X_{ms} = X_{mu}$ i.e. under unsaturated magnetic conditions.

Using equations 5.1 and 5.4, the equation 4.4 can now be written as

$$T = \frac{I_1^2 \left(\frac{R_2}{S}\right)}{\frac{\left(\frac{R_2}{s}\right)^2}{X_{ms}^2} + \frac{(X_{mu} + X_2)^2}{X_{mu}^2}} \qquad 5.5$$

The equation 2.7 can be written as

$$T = \frac{I_1^2 \left(\frac{R_2}{S}\right)}{\frac{\left(\frac{R_2}{S}\right)^2}{X_m^2} + \frac{(X_m + X_2)^2}{X_m^2}} \qquad 5.6$$

Now the maximum value of X_m will be equal to X_{mu}, pessimistic. It can be noticed that the critical speed is directly defined by equation 5.6 in the case of synchronous impedence method.

A study of the equations 5.6 and 5.5, thus makes it abundently clear that under saturated conditions a drastic disparity of the results by the two methods can be expected in the region of the maximum torque, and inherently deviating results in the other speed ranges. Then the question arises as to which of the methods is correct or whether both are inaccurate. Definitely and undoubtedly the induction motor method is a convincing analysis of the problem and has given the due consideration for the complex magnetic saturation with judicially chosen simplified assumptions, the validity of the results of which have been fully supported by wide range of test results by many authors[18,20,22,24]. Only LaPierre and Metaxas[13] have used the synchronous impedence method but only to meet with inaccurate results.

Actually in the machine the resultant air gap flux established after taking into account the reaction of the rotor currents on the stator flux, can reasonably determine the extent of saturation. In the induction motor method it is the value of the air gap flux in terms of the airgap voltage V_2, that determines the condition of magnetic saturation, and the value of the magnetizing reactance is defined accordingly, and proper values of X_m as defined by the airgap voltage V_2 and the open circuit characteristic are used in the equations 2.1 to 2.7, in order to convincingly justify the effects of saturation.

In the synchronous impedence method the effect of the rotor m.m.f. is taken as a voltage drop straightway through the parameter X_s and assumed to be directly proportional to the rotor current, Similarly the effect of the stator m.m.f. taken separately, is determined as an induced voltage. Then the resultant performance conditions are determined without the knowledge of the airgap voltage. Thus in the presence of saturation the method becomes basically incorrect.

In order to effect a direct comparison of the results by the induction motor method and the synchronous impedence method adopted by LaPierre and Metaxas[13], the torque/speed characteristics of the slip-ring motor mentioned in table 2.2 have been calculated by both the methods, from the test data published by Butler[22]. Referring to figure 5.1, curve A is that for an excitation current $I_1 = 4$ per unit, calculated by using the former method. Curve B shows the characteristic for the same value of excitation calculated by the synchronous impedence method. Similarly the curves C and D are for an excitation $I_1 = 2$ per unit, by using the former and latter methods respectively. All the calculated values of the torques and speeds are tabulated in Tables 5.1a and 5.1 b. It can be readily seen that there is a drastic deviation of the results obtained by the two methods. It is worthwhile pointing out that the results obtained by the induction motor method on the machine under consideration, have been experimentally verified to be within reasonable accuracy. Thus the synchronous impedence method gives results which are very much inaccurate and the nature of the deviation is almost to our expectation with the

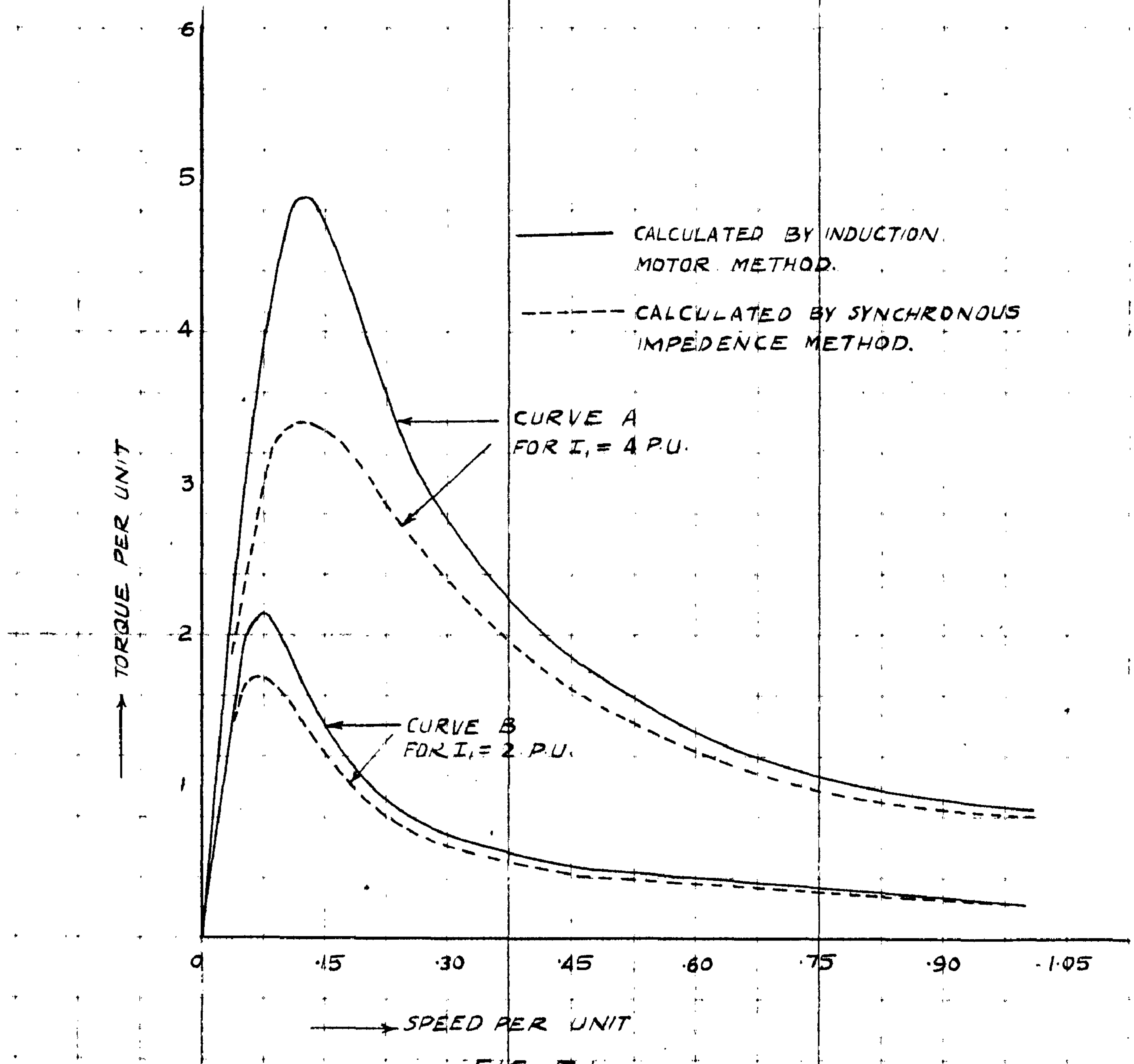

FIG. 5·1

SPEED-TORQUE CHARACTERISTICS OF AN INDUCTION MOTOR. (DETAILS OF MOTOR GIVEN IN TABLE NO. 22.)
A COMPARISON BETWEEN INDUCTION MOTOR METHOD AND SYCHRONOUS IMPEDENCE METHOD.

TABLE [illegible] THE CALCULATED VALUES OF TORQUES AND SPEEDS BY THE INDUCTION MOTOR METHOD, SYNCHRONOUS IMPEDENCE METHOD, AND THE MODIFIED SYNCHRONOUS IMPEDENCE METHOD, FOR THE DYNAMIC BRAKING OPERATION OF THE MOTOR WHOSE DETAILS ARE GIVEN IN TABLE 4.2

$I = 55$ AMPS $= [illegible]$ PU ; $E_2 = [illegible]$ VOLTS.

$X_s = 40\ [illegible]$, $R_2 = 0.27\ \Omega$, $X_2 = 0.56\ \Omega$

LOAD POINTS	1	2	3	4	5	6	7	8	9	10
SPEED PER UNIT X100	2.0[illegible]	[illegible]32	4.[illegible]4	6.[illegible]	[illegible].95	8.25	[illegible]4	20	50	[illegible]00
TORQUE PER UNIT (INDUCTION MOTOR METHOD)	[illegible]895	14[illegible]	[illegible]6	[illegible]09	2.[illegible]	2.[illegible]	1.715	[illegible]01	0.4[illegible]	0.206
TORQUE PER UNIT (SYNCHRONOUS IMPEDENCE METHOD)	0.84	[illegible]9	44	[illegible]46	[illegible]56	48	[illegible]28	0.[illegible]95	0.[illegible]0	0.201
TORQUE PER UNIT (MODIFIED SYNCHRONOUS IMPEDENCE METHOD) $X_{ms} = 5.02$	1.39	[illegible]	[illegible]00	[illegible]	[illegible]82	179	150	0.[illegible]8	[illegible]41	0.205

TABLE 5.1 (b)

$I = [illegible]93$ AMPS $= 4$ PU , $E_2 = 239$ VOLTS,

$X [illegible] 23\ \Omega$, $R_2 = 0.27\ \Omega$, $X_2 = 0.5[illegible]\ \Omega$

LOAD [illegible]	1	2	3	4	5	6	7	8	9	[illegible]0	
SPEED PER UNIT X100	[illegible]7	92	3.62	[illegible]9	2.85	[illegible]	[illegible]	[illegible]3	4.5	7[illegible]	[illegible]
TORQUE PER UNIT (INDUCTION MOTOR METHOD)	7[illegible]	[illegible]9	[illegible]02	4.[illegible]8	4.89	4.63	4.23	3.[illegible]6	2.04	1.13	[illegible]
TORQUE PER UNIT (SYNCHRONOUS IMPEDENCE METHOD)	[illegible]	[illegible]	[illegible]	3.25	3.40	3.[illegible]9	[illegible]	2.[illegible]8	[illegible]82	[illegible]09	[illegible]
TORQUE PER UNIT (MODIFIED SYNCHRONOUS IMPEDENCE METHOD)	[illegible]32	[illegible]	[illegible]	[illegible]	4.25	3.9[illegible]	3[illegible]	2.88	[illegible]90	[illegible]	[illegible]

form of equation 5.5 specially derived to effect a direct comparison. LaPierre and Metaxas have presented the method with a reference to squirrel-cage motors, but if their method is theoretically sound it should not result in such a pronounced deviation from the actual values, if applied to a slip-ring induction motor as well. It must be pointed out that LaPierre and Metaxas themselves have obtained very much inaccurate results by using the synchronous impedence method on a squirrel-cage motor tested by the authors[13].

The value of the synchronous impedence X_s used by LaPierre and Metaxas[13] corresponds to an excitation of the full stator exciting current I_1 which is the most severe condition of magnetic saturation for the particular stator current chosen. This at once suggests whether any compromised situation of the saturated conditions can be chosen to evaluate X_s. But analysing the equation 4.4 it can be noticed that in case X_s is increased without changing the value of E_2, decreased torque values will result all through the speed range. In case E_2 is changed the co-relation between the value of stator exciting current and the torque values may be lost. Thus equation 5.5 is better suited to analyse the possibilities of taking a compromised value of X_{ms}. An empirical estimate of taking the value of X_{ms} at 70% of the exciting current has been arrived at, which will give closer agreement between the calculated values and test results. Fig. 5.2 shows the curves as calculated by the induction motor method and the modified synchronous impedence method for an excitation current $I_1 = 4$ P.U. as well as for a value of $I_1 = 2$ P.U. for the same motor mentioned in Table 2.2. The calculated values of torques and speeds are given in

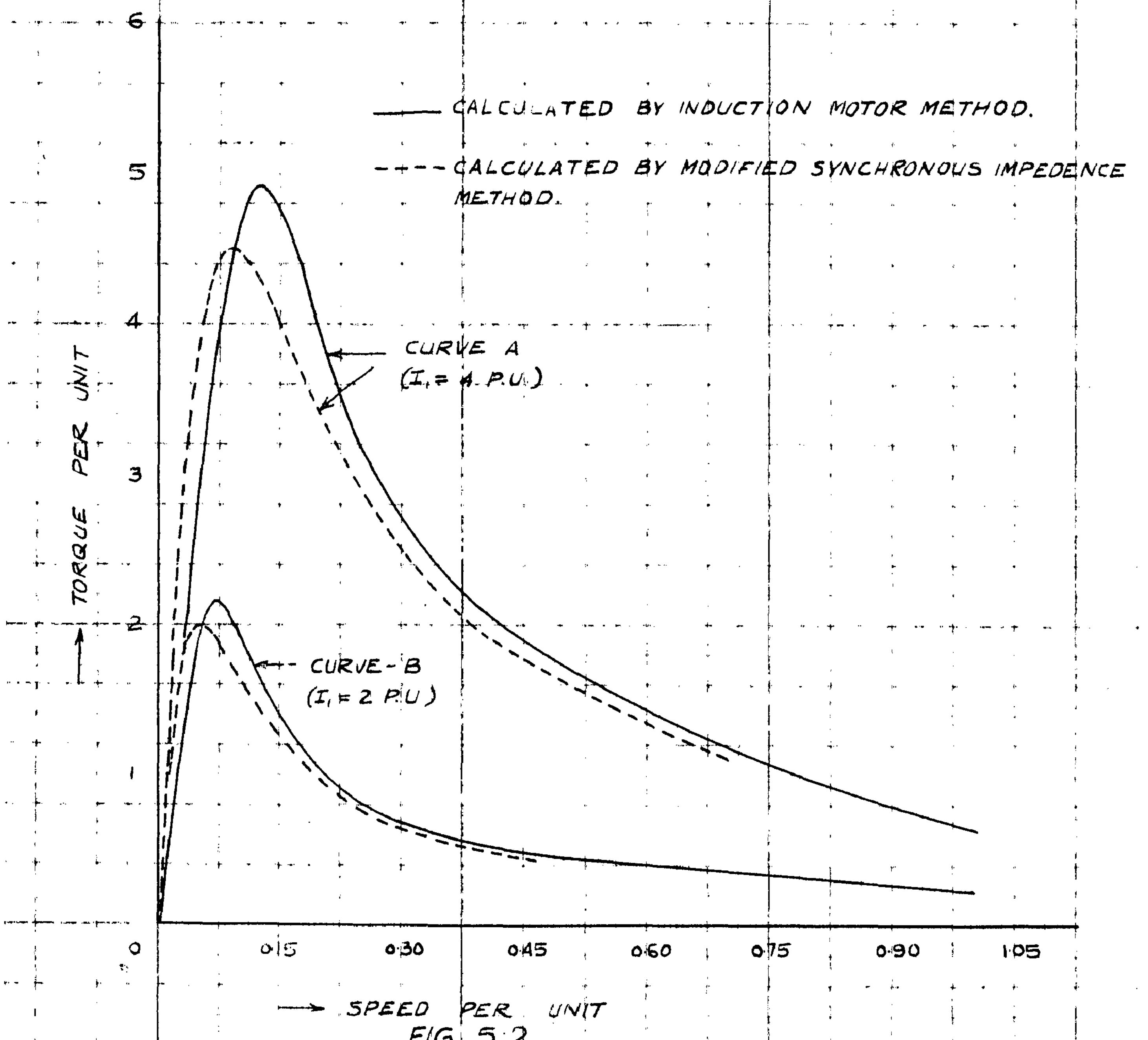

FIG. 5.2

TORQUE-SPEED CHARACTERISTICS OF AN INDUCTION MOTOR (MOTOR DETAILS GIVEN IN TABLE NO. 2.2). A COMPARISON BETWEEN INDUCTION MOTOR METHOD AND MODIFIED SYNCHRONOUS IMPEDENCE METHOD.

Tables 5.1a and 5.1 b. Even so, it can be seen that disparity in the results still persist appreciably. The stable portion is distorted to give higher values of torque, though the unstable portion is in closer agreement. But as the area under the unstable portion is mainly the criterion for determining the stopping time for normal values of rotor resistances, the method perhaps could be used to evaluate the stopping time approximately.

But whether a compromised value of X_{ms} is chosen or not, it can anyway be clearly concluded that the synchronous impedence method cannot give due consideration for the effects of saturation. Having used a constant value of "adjusted synchronous reactance" over the whole of the speed range, for a particular reactance" over the whole of the speed range, for a particular value of excitation, inaccuracy has been introduced not only in the region in which saturation is present but also in the unsaturated regions of operation. There is evidently a continuous variation of the extent of saturation under normal braking conditions and as such it is impossible to express the value of the torque in terms of the speed with constant values of parameters as has been done in equation 4.4, without introducing considerable inaccuracy in the results. This amounts to the representation of the magnetization curve by a linear equation which is impossible for normal values of stator excitation.

In order to further investigate the validity of the induction motor method as compared to the synchronous impedence method of analysis for calculating the d.c. braking performance of an induction motor, the torque/speed characteristics have been calculated using both the methods for the squirrel-cage motor tested by LaPierre and Metaxas[13]. The details of the motor are given in Table 5.2 and the magnetization curve of the motor is shown in figure 5.3.

TABLE 5.2

SQUIRREL CAGE MOTOR

5 h.p.; 220 volts; 3 phase; 60
Synchronous speed: 1200 R.p.m.
Rated current:- 15 amps
Rated Torque :- 22.5 lbs.ft.
R_2 = .6 ohms/phase
X_2 = .9 ohms per phase
Open circuit characteristic:-Refer figure 5.3
Motor data compiled from the paper by LaPierre and Metaxas[13]

Figure 5.4 shows the torqe/speed characteristics calculated by both the methods for the motor whose details are given in Table 5.2. Curves A are for an exciting current I_1 = 1.635 per unit and curves B are for I_1 = 1.085 per unit. The experimental curves as obtained by LaPierre and Metaxas are also clearly indicated by dotted lines in the figure. The calculated values of the torques and speeds are tabulated in tabular forms 5.3a and 5.3b for the two values of excitation. It is immediately clear that the induction motor method is much more accurate than the synchronous impedence method. The slight deviation of the results obtained by the induction motor method and the experimental values, in the region of maximum torque, can be

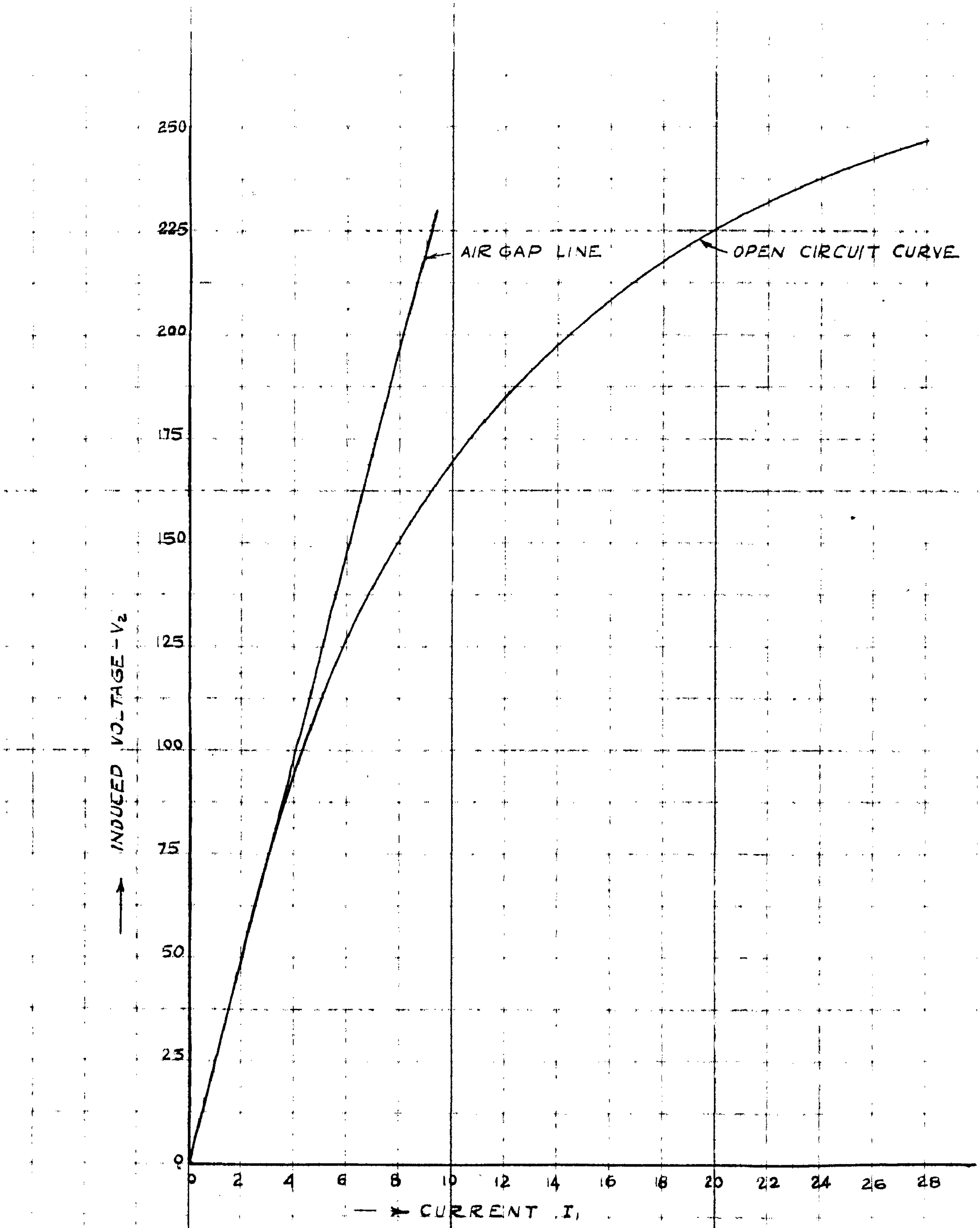

FIG. 5·3

OPEN CIRCUIT CHARACTERISTIC OF THE MACHINE WHOSE DETAILS ARE GIVEN IN TABLE NO

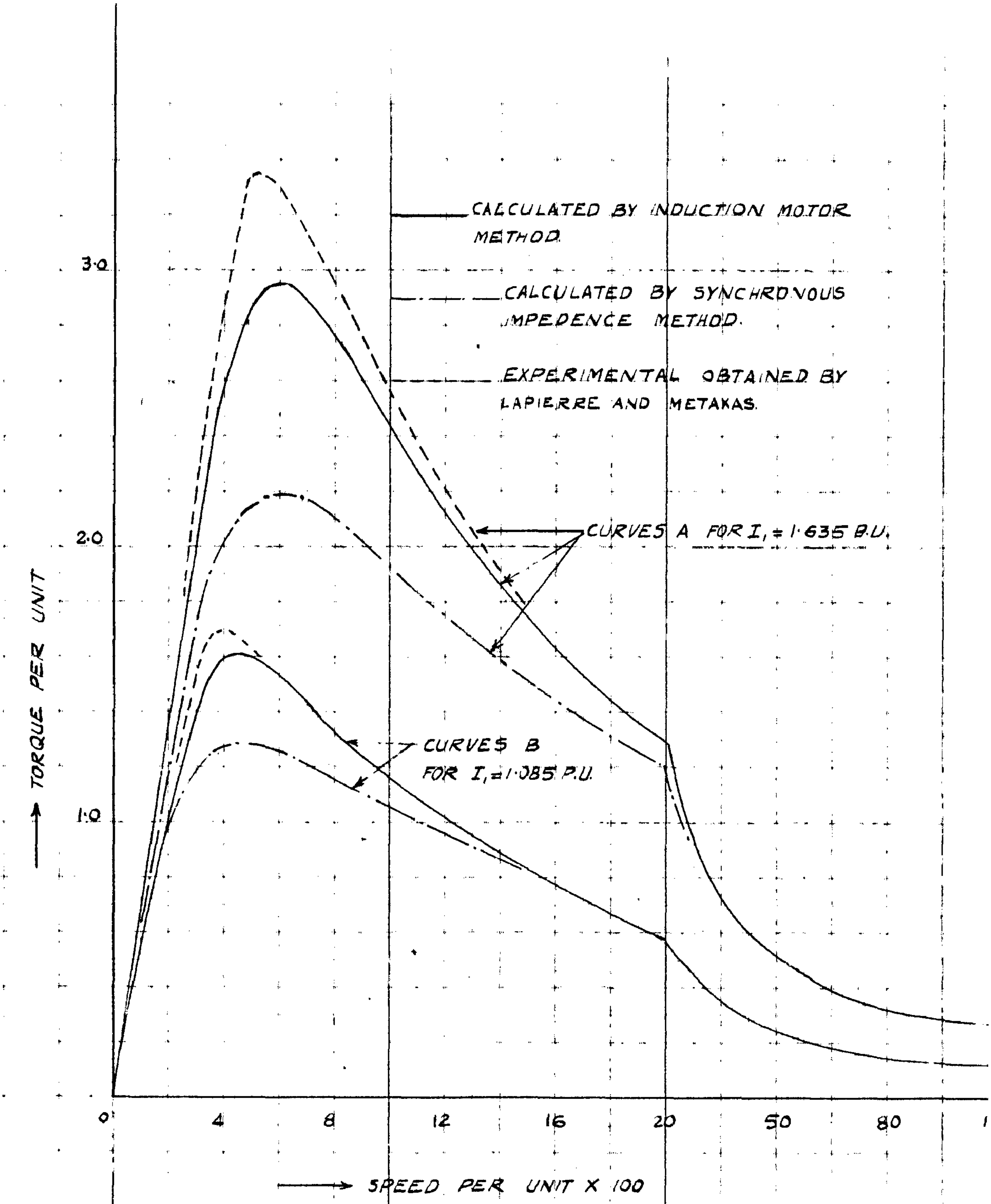

FIG. 5·4

TORQUE SPEED CHARACTERISTICS OF A SQUIRREL CASE INDUCTION MOTOR UNDER DYNAMIC BRAKING (MOTOR DETAILS GIVEN IN TABLE NO.
A COMPARITIVE STUDY OF RESULTS BY INDUCTION MOTOR METHOD AND SYNCHRONOUS IMPEDENCE METHOD.

TABLE NO 53(a)

TABLE SHOWING THE CALCULATED VALUES OF TORQUE AND SPEED BY THE INDUCTION MOTOR METHOD AND THE SYNCHRONOUS IMPEDENCE METHOD FOR DYNAMIC BRAKING CONDITIONS OF A SQUIRREL CAGE INDUCTION MOTOR (MOTOR DETAILS ARE GIVEN IN TABLE NO 5)

I = 24.3 AMPS = 1635 PU, R_2 = 06 Ω,

X_2 = 09 Ω, E_2 = 238 VOLTS, X_S = 101 Ω.

LOAD POINTS	1	2	3	4	5	6	7	8	9	10	11	12
SPEED PER UNIT X 100	2	3.1	4.3	5 7	6 13	6 6	7 6	0 8	16.6	41 7	75	100
TORQUE PER UNIT CALCULATED BY INDUCTION MOTOR METHOD	·44	209	2.62	294	295	292	2 62	2 27	.38	63	55	264
TORQUE PER UNIT CALCULATED BY SYNCHRONOUS IMPEDENCE METHOD	[illegible]	18	2.07	2 18	2.19	2.8	2 13	1 37	76	6	445	26

TABLE 53 (b)

I_1 = 16 3 AMPS = 065 PU, R_2 = ·[illegible] Ω

X_2 = 9 Ω, E_2 = 405 VOLTS, X_S = [illegible] Ω

LOAD POINTS	1	2	3	4	5	6	7	8	9	10	11	12
SPEED PER UNIT X 100	[illegible]	2 35	3 3	4.0	4 75	6 05	7 9	9 6	25	50	75	100
TORQUE PER UNIT CALCULATED BY INDUCTION MOTOR METHOD.	·965	1 22	·49	·5	1 59	1 55	1 53	1 15	·465	231	1 35	1 16
TORQUE PER UNIT CALCULATED BY SYNCHRONOUS IMPEDENCE METHOD.	·875	1 16	1 25	1 27	1 25	24	1 11	104	·455	23	[illegible]	1 4

CHAPTER -6

MACHINE PERFORMANCE UNDER D.C. DYNAMIC BRAKING CONDITIONS - THE POTIER TRIANGLE METHOD OF ANALYSIS

due to the effect of slot harmonics. As compared to the induction motor method the torque values calculated by the synchronous impedence method are considerably deviating from the test values. LaPierre and Metaxas[13] have tried to explain off all the discripencies in the results by using their method, to be that due to the harmonic induction torques. Normally for an induction motor the effect of slot harmonics is small and cannot alone account for the pronounced deviation of the results obtained by the synchronous impedence method from the actual torque produced. As explained before such a pronounced deviation is only due to the inadequate and improper treatment of the saturation effects in the synchronous impedence method.

In contrast to the synchronous impedence method, the induction motor method of analysis, is theoretically sound, having given a justified treatment for the effects of saturation. The experimental results obtained agree very closely with the latter method and has been verified by many authors[19,20,22]. Even in conventional alternator calculations the synchronous impedence method has never given accurate results and applying the method for an induction motor under d.c. braking with a continuous change in speed, frequency and the extent of saturation, is far from satisfactory. It is interesting to point out that the induction motor approach suits more admirably the dynamic braking performance of the machine than the motoring performance itself, having given consistently accurate results for d.c. braking. Thus the induction more method is more suitable, adaptable and accurate for calculation of the d.c. braking performance of an induction motor, than the synchronous impedence method.

CHAPTER - 6

MACHINE PERFORMANCE UNDER D.C. DYNAMIC CONDITIONS - THE POTIER TRIANGLE METHOD OF ANALYSIS

Cochran[15] has given a method to calculate the dynamic braking characteristics of a wound rotor induction motor using a modified zero power factor saturation curve method as applied to alternator calculations. As presented by Cochran the calculations are based on design data and so far the method has not been supported by published test results on an existing machine. Commenting on Cochran's method, Butler[24] states that "the method has not been compared with test results and cannot be expected to provide extreme accuracy". Harrison[20] states that the method is tedious to apply, which statement is absolutely correct. The method as put forward by Cochran is extremely laborious and cumbersome for effecting the calculations of the d.c. braking performance of an induction motors.

Here, it is proposed to present Cochran's method in a modified form and simplified equations are evolved to make the analysis an easier proposition.

The open circuit characteristic of the machine is first of all determined at the synchronous speed, as explained in article 2.4.3.

The next step is to determine the Potier triangle which can be obtained as follows. Referring to figure 6.1, OM is the open circuit characteristic of the machine and ABC is the Potier triangle. The side BC of the triangle, is the stator excitation current required to overcome the demagnetising effect of the

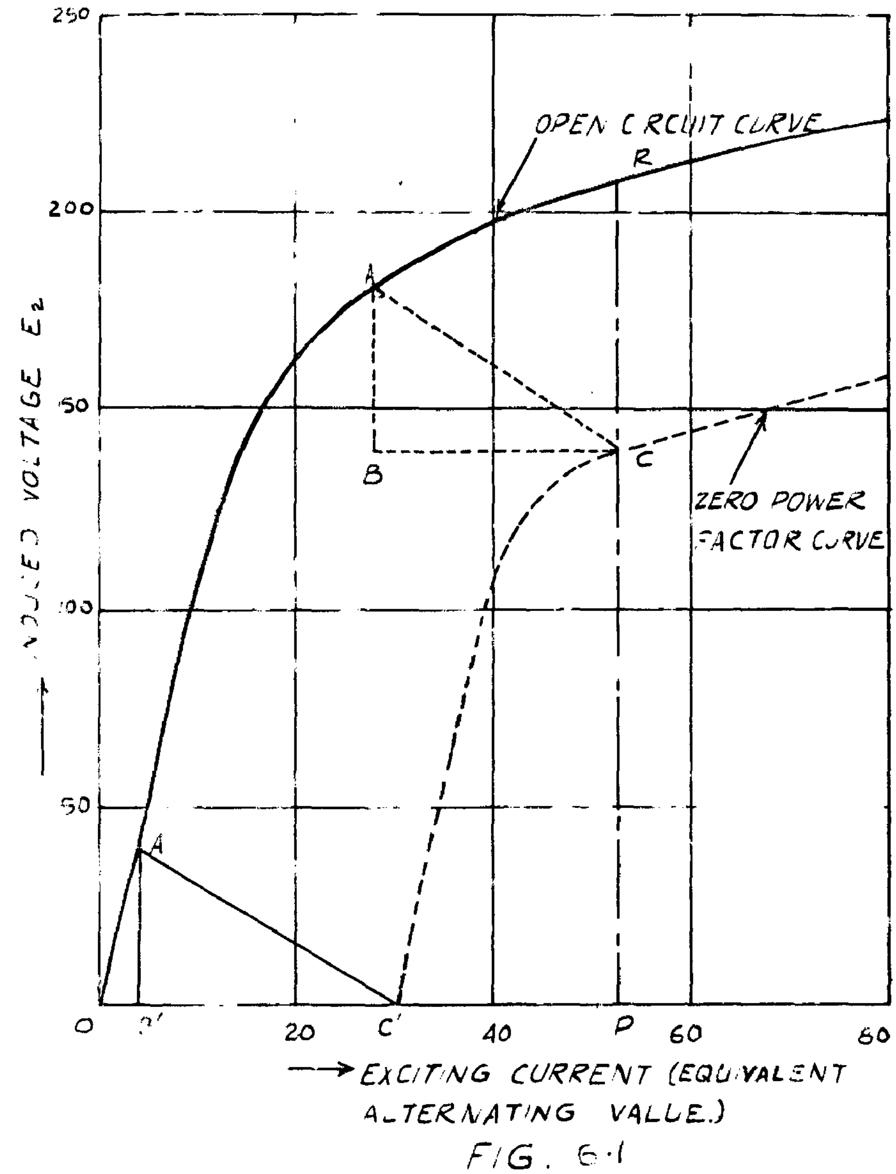

OPEN CIRCUIT CURVE
R
A
B
C
ZERO POWER FACTOR CURVE
A
250
200
150
100
50
O
B'
20
C'
40
P
60
80
INDUCED VOLTAGE E_2
EXCITING CURRENT (EQUIVALENT ALTERNATING VALUE.)

FIG. 6·1

rotor current under the zero power factor conditions. This will be exactly equal to the rotor current I_2 (referred to the stator) because the open circuit characteristic (in the case of an induction motor) shows the relationship between the air gap voltage V_2 and the equivalent alternating current of the stator direct current excitation. The altitude AB of the triangle is the rotor leakage reactance drop I_2 X_2, keeping in mind that X_2 is also referred to the stator. Thus the Potier triangle can be evolved for a particular value of I_2, the assumption being that the sides of the Potier triangle are proportional to the current I_2. Hence it is assumed that saturation does not affect the size of the Potier triangle, which is a reasonable assumption.

By moving the Potier triangle such that the point A' traces the path along the open circuit curve, with the base always horizontal, the zero power factor characteristic for a particular value of I_2 is obtained which is the path traced by the point C' of the triangle.

For a particular value of stator excitation I_1 = OP (Refer figure 6.1), the vertical intercept RC between the open circuit curve and the zero power factor characteristic for a particular value of I_2, will give the combined voltage drop due to the leakage reactance X_2 and the effect of the rotor current on the stator flux. Thus the intercept RC is equal to I_2 X_s where X_s is the synchronous reactance at point C. The synchronous reactance X_s causes the induced voltage RP to be reduced to CP at the zero power factor conditions.

Comparing the rotor of the induction motor under braking to the armature of an alternator, it is assumed that the rotor resistance R_2 is acting as the load and the terminal voltage is E_{2R} which is the drop across the resistance R_2. Thus as far as the voltage E_{2R} is concerned the current I_2 is always at unity power factor independent of the relative magnitude of R_2 and X_2. Now an important assumption is made, which takes the synchronous impedence drop $I_2 X_s$ to be the same in magnitude for zero as well as unity power factor conditions, for the same magnitude of I_2. Thus the change in the extent of saturation for the same magnitude of I_2 but at different power factors, is neglected. It must be noted that the resistance of the rotor circuit has been separated out as a load and the zero power factor curve is purely imaginary. If the current were at unity power factor the terminal voltage E_{2R} (which is the drop across R_2), added at right angles to the synchronous impedence drop $I_2 X_s$ should give the induced voltage E_2 = RP. Hence for a particular value of current I_2, with the stator excitation I_1 = OP we get

$$E_{2R} = \sqrt{E_2^2 - (I_2 X_s)^2} \qquad 6.1$$

Choosing different points on the zero power factor curve, the corresponding points on the unity power factor curve can be obtained. Thus the unity power factor curve for a particular value of I_2, is computed.

Now the entire procedure is repeated for getting the unity power factor curves for different values of I_2. Then for a particular chosen value of stator excitation the equations for torque/speed relations are obtained as follows.

For the value of excitation I_1 chosen, the rotor resistance drop E_{2R} at the synchronous speed, for an assumed value of rotor current I_2 is obtained from the unity power factor curve for current I_2.

Hence at any other speed N the rotor resistance drop will be

$$e_{2R} = \frac{N}{N_s} E_{2R} \qquad 6.2$$

But the actual voltage drop e_{2R} at speed N is also given by

$$e_{2R} = I_2 R_2 \qquad 6.3$$

Hence from equations 6.2 and 6.3 the value of speed N can be determined. Then the torque is synchronous watts will be

$$T = m \cdot I_2^2 R_2 \left(\frac{N_s}{N}\right) \qquad 6.4$$

The torque speed characteristic can then be plotted for the particular value of I_1, by repeating the above procedure for various values of I_2.

So far the method has been described so as to have the theoretical aspects involved in the procedure. In practice it is not necessary to draw the zero power factor and unity power factor curves, and the method can be further simplified as below.

The open circuit curve is first obtained as shown in figure 6.1. Suppose the dynamic braking characteristics are to be determined at a particular value of stator excitation $I_1 = OP$, then the induced voltage $E_2 = RP$, is obtained from the open circuit curve for the excitation $I_1 = OP$. Choose any point A on the open circuit curve as shown. The values V_a and I_a which are the voltage and current at the point A of the open circuit curve are noted down. Then the value of I_2 can be obtained from

$$I_2 = I_1 - I_a \text{ (because } I_2 = BC) \qquad 6.5$$

The rotor resistance drop at synchronous speed is given by

$$E_{2R} = \sqrt{E_2^2 - (E_2 - V_a + I_2 X_2)^2}$$

$$= \sqrt{(V_a - I_2 X_2)\ (2E_2 - V_a + I_2 X_2)} \qquad 6.6$$

Hence the speed is given by (from equations 6.2 and 6.3)

$$\frac{N}{N_s} = \frac{I_2 R_2}{E_{2R}} \qquad 6.7$$

and the torque in synchronous watts will be

$$T = m\ I_2^2\ R_2 \frac{N_s}{N} = m\ E_{2R}\ I_2 \qquad 6.8$$

Choosing various points A on the open circuit curve, the torque/speed characteristic can be readily computed by using the equations 6.5 to 6.8. It can be seen that the equations 6.5 to 6.8 are simple as compared to equations 2.1 to 2.7.

CHAPTER - 7

DISCUSSION AND COMPARISON OF THE POTIER TRIANGLE METHOD AND THE INDUCTION MOTOR METHOD AS APPLIED TO THE D.C. BRAKING OF INDUCTION MOTORS

CHAPTER-7

DISCUSSION AND COMPARISON OF THE POTIER TRIANGLE METHOD AND THE INDUCTION MOTOR METHOD AS APPLIED TO THE D.C. BRAKING OF INDUCTION MOTORS

7.1. Discussion and comparison of the Potier Triangle Method and the Induction Motor Method.

In order to effect a direct comparison of the Potier triangle method and induction method, as applied for calculating the d.c. dynamic braking performance of an induction motor, it will be advisable to modify the equations 6.5 to 6.8 of the Potier triangle method, so that the equations are reduced to similar form in both the methods.

Taking the value of the magnetising reactance at the point A on the open circuit curve (Figure 6.1) as X_{ma}, and the value corresponding to $I_1 = OP$ as X_{ms}, the equations 6.6 and 6.7 can be solved to get the value of I_2 in terms of I_1, X_{ms}, X_{ma}, R_2 and S.

The quadratic equation thus obtained is:

$$I_2^2 \left(\frac{R_2}{S}\right)^2 + (X_{ma} + X_2)^2 - 2\, I_1\, I_2\, (X_2 + X_{ma})\, (X_{ms} - X_{ma})$$
$$+\, I_1^2 \quad X_{ma}^2 - 2\, X_{ms}\, X_{ma} \quad = \quad 0 \qquad 7.1$$

Solving the above quadratic equation we get

$$I_2 = I_1 \frac{\left[X_{ma} + X_2\right]\left[X_{ms} - X_{ma}\right] + \sqrt{X_{ms}^2 (X_2 + X_{ma})^2 + \frac{R_2^2}{S^2}\left(2 X_{ms} X_{ma} - X_{ma}^2\right)}}{\left(\frac{R_2}{S}\right)^2 + (X_2 + X_{ma})^2} \qquad 7.2$$

It may be noted that the positive root has been chosen because according to our assumption I_2 is positive.

Then the torque value will be given by $T = I_2^2 \frac{R_2}{S} \times m$ as before.

Equation 2.3a obtained by the induction motor method is written down below for convenience.

$$I_2 = I_1 \frac{X_m}{\sqrt{(\frac{R_2}{S})^2 + (X_2 + X_m)^2}} \qquad 2.3a$$

where X_m is the value of the magnetizing reactance at a point on the open circuit curve corresponding to a value of I_m assumed.

The equations 7.2 and 2.3a, are strikingly similar. But it should be noted that X_m and X_{ma} can values corresponding to different points on the open circuit curve. Suppose X_m is also taken at point A, even so, it can be seen that the current values obtained and hence the torque values calculated by both the methods can be different. But if there is no saturation upto a value of current equal to I_1 in the open circuit curve, we get

$$X_{ms} = X_{ma} = X_{mu}$$

Thus under unsaturated magnetic conditions, it can be readily seen that the equations 7.2 and 2.3a become exactly identical. Hence the main difference of the Potier triangle method and the Induction Motor Method, lies in the manner in which saturation is accounted for. This depends on the assumptions based on which the procedures are adopted. In the Potier triangle method it has been assumed that the extent of saturation, varying with the power factor of I_2 is negligible, in order to easily compute the unity power factor curve. Also the effect of saturation on the size of the Potier triangle has not been considered. Usually both the effects are small and negligible error is introduced by the assumptions involved. In the Induction motor method, the air gap flux is assumed to determine the extent of saturation which, as explained in Chapter 5, is a reasonable assumption. Hence as such, it can be expected that somewhat close agreement of the results can be forthcoming for ordinary induction motors by these two methods. For evaluating the torque and speed, points on the open circuit curve for different values of I_m are chosen in the case of the induction motor method, whereas points corresponding to a value of (I_1-I_2) are chosen in the Potier triangle method. As such an identical result may not be obtained in the presence of magnetic saturation. A direct comparison of equations 7.2 and 2.3a, is not feasible under conditions of magnetic saturation, due to the involvement of a non-linear saturation curve and as such only the calculated results shall be the proper resort for an effective comparison.

Using the test data on the slip ring motor whose details are given in table 2.2, the torque/speed characteristics have been computed using the Potier triangle method.

Figure 7.1 shows the torque/speed characteristics obtained by using both the methods, for two values of the exciting current curve A for I_1 = 4 per unit and curve B for I_1 = 2 per unit. The results obtained by both the methods are so very close, that the same curve can represent the characteristic. Points calculated by each of the method are individually marked on the curve. Also the calculated values of the torques and speeds are tabulated in

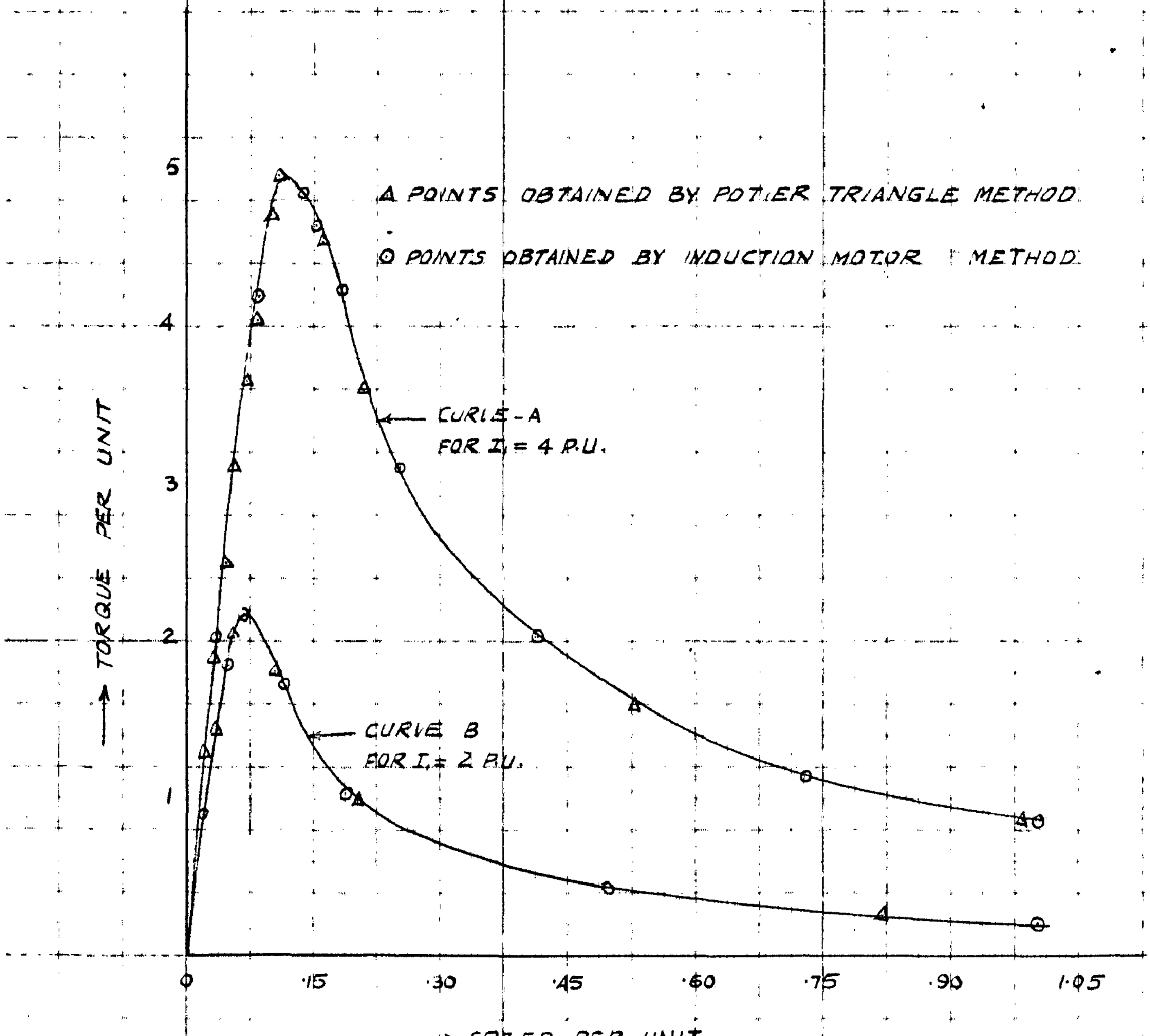

FIG. 7·1

TORQUE-SPEED CHARACTERISTICS OF AN INDUCTION MOTOR (DETAILS OF MOTOR GIVEN IN TABLE NO 2.2) UNDER DYNAMIC BRAKING-COMPARISON BETWEEN POTIER TRIANGLE METHOD AND INDUCTION MOTOR METHOD.

TABLE 7.1(a)

TABLE SHOWING THE CALCULATED VALUES OF TORQUE BY THE POTIER TRIANGLE METHOD FOR DYNAMIC BRAKING OF AN INDUCTION MOTOR (MOTOR DETAILS ARE GIVEN IN TABLE 2.2

$I_1 = 56$ AMPS $= 2$ P U, $E_2 = 212$ VOLTS,

$R_2 = \cdot 27\ \Omega$; $X_2 = \cdot 56\ \Omega$

LOAD POINTS	1	2	3	4	5	6	7	8
SPEED PER UNIT	0205	·0353	0478	060	072	·099	·196	·32
TORQUE PER UNIT AS CALCULATED BY POTIER TRIANGLE METHOD	·69	1·43	1·875	2·13	2·10	1·765	1·0	[illegible]

THE TORQUE VALUES CALCULATED BY USING THE INDUCTION MOTOR METHOD ARE GIVEN IN TABLE 7.1(a)

TABLE 7.1(b)

$I_1 = 112$ AMPS. $= 4$ P U., $E_2 =$ [illegible] VOLTS

$R_2 = \cdot 27\ \Omega$, $X_2 = \cdot 56\ \Omega$

LOAD POINTS	1	2	3	4	5	6	7	8		
SPEED PER UNIT	023	034	·046	071	096	117	150	[illegible]	[illegible]	[illegible]
TORQUE PER UNIT AS CALCULATED BY POTIER TRIANGLE METHOD		[illegible]	2·51	[illegible]	4·7	4·[illegible]	4·51			[illegible]

[illegible] VALUES CALCULATED [illegible] THE [illegible] GIVEN IN TABLE 7.1(b)

Tables 7.1a and 7.1b. It is evident from the results obtained that the Potier triangle method also gives as accurate results as the induction motor method of analysis.

In order to further investigate the reliability of the Potier triangle method and the associated equations 6.5 to 6.8 presented in this dissertation, calculations have been made by the above method on the squirrel cage motor whose test data are given in table 5.2. The results obtained by using each of the two methods, are presented in graphical form in figure 7.2. The calculated values of the torques and speeds are tabulated in table 7.2a and 7.2b.

Referring to figure 7.2, curve A shows the relationship between torque and speed for a value of I_1 = 1.635 per unit; and curve B is for a value of I_1 = 1.085 per unit. The points obtained by the Potier triangle method and the induction motor method are marked clearly on the figure. The results obtained by both the methods are so very close that the same curve can be used to represent both the results. The dotted lines are the experimental curves as determined by LaPierre and Metaxas on the motor under consideration. It can be seen that both the Potier triangle method and the induction motor method give almost identical results. But both the methods give maximum errors of 12% and 8% for curves A and B respectively in the region of maximum torque. As explained in Chapter 5, this can be due to the slot harmonics whose effects are not considered in either of the methods. Thus considering the assumptions involved in the methods, the results obtained are quite satisfactory. Also it is clear from figure 5.4, that the results obtained on the same motor by using the synchronous impedence method are in error to the extent of 31% and 23% for curves obtained for

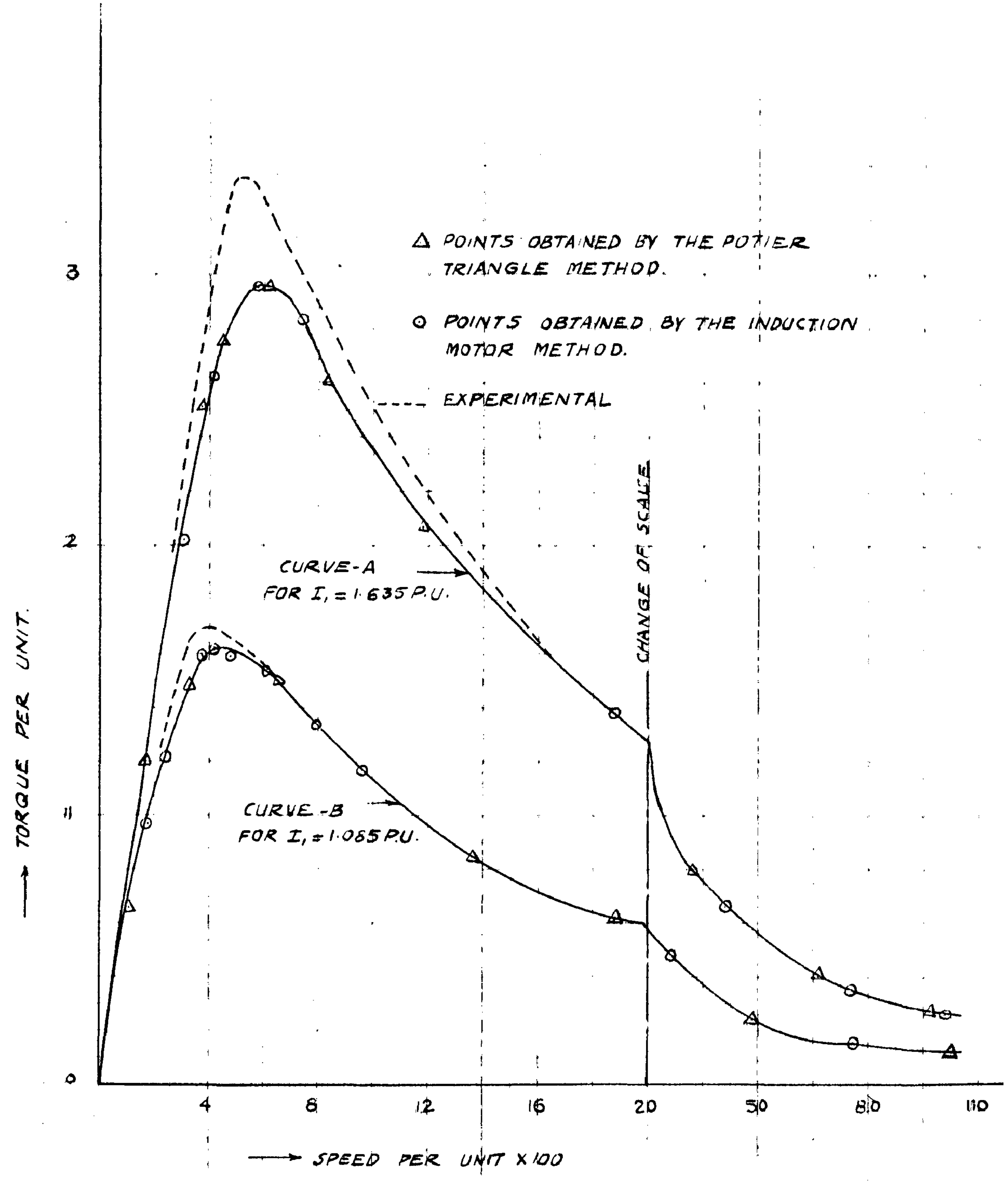

FIG. 7·2

TORQUE-SPEED CURVES OF A SQUIRREL-CAGE INDUCTION MOTOR UNDER DYNAMIK BRAKING (MOTOR DETAILS ARE GIVEN IN TABLE NO. POINTS CALCULATED BY THE POTIER TRIANGE METHOD AND THE INDUCTION MOTOR METHOD ARE SEPARATELY SHOWN.

[illegible] 7·2 [illegible]

[illegible] THE [illegible] VALUES OF TORQUE [illegible] BY POTIER TRIANGLE METHOD FOR DIFFERENT LOADING CONDITIONS OF THE SQUIRREL CAGE [illegible] 10102 WHOSE DETAILS ARE GIVEN IN TABLE NO 5 2

I_1 = [illegible] 3 AMPS = ·085 P.U., R_2 = 6 Ω,
X_2 = 9 Ω, E_1 = 209 VOLTS

LOAD POINTS	1	2	3	4	5	6	7	8	9	10	11	12
SPEED PER UNIT × 00	·15	·75	3 28	3 75	4 1	5 33	6 5	5 7	[illegible]	[illegible]	77	102
TORQUE PER UNIT CALCULATED BY POTIER TRIANGLE METHOD	65	565	1 48	1 5	1 62	·56	49	829	5 5	·23	5	[illegible]

THE VALUES OF TORQUES AND SPEEDS CALCULATED BY THE INDUCTION MOTOR METHOD ARE GIVEN IN TABLE 5·5(b)

TABLE 7·2 (b)

I = [illegible] AMPS = [illegible] P.U., E = [illegible] VOLTS
[illegible] 6 Ω, X = [illegible] 9 Ω

LOAD POINTS	[illegible]	2	3	4	5	6	7	8	[illegible]	[illegible]	[illegible]	[illegible]
SPEED PER UNIT × [illegible]	·65	2 57	3 77	4 48	6 13	6 78	7 17	8 35	1 8	[illegible]	[illegible]	[illegible]
TORQUE PER UNIT CALCULATED BY POTIER TRIANGLE [illegible]	2	[illegible]	431	274	[illegible]	[illegible]	307	283	[illegible]	208	[illegible]	[illegible]

THE [illegible] TORQUES AND SPEEDS [illegible]

[illegible]

the two values of exciting currents $I_1 = 1.635$ and $I_1 = 1.085$ per unit, respectively. This makes it abundently clear that the Potier triangle method and the induction motor method are by far the most accurate and simple methods to predict the torque/speed curves under d.c. dynamic braking of an induction motor.

7.2 Conclusion.

In spite of introducing more assumptions for accounting for the effects of saturation, accuracy of the results obtained by the Potier triangle method, only adds to the justification of the assumptions. As compared to the Potier triangle method and the induction motor method, the synchronous impedence method is far from satisfactory both from the point of view of the theoretical basis as well as the practical results. Hellmond's method of analysis can be evidently seen to be out of date as compared to the later simplified solutions of the problem. In all the methods discussed we have been able to present the equations in a strikingly similar form. Under unsaturated magnetic conditions all the methods become exactly identical, which is only a natural and justified expectation. In all the methods of analysis of the problem, it can be seen that a procedure is adopted based on certain assumptions. The ability of the engineer lies in the interpretation of an apparently complex problem, into a comparatively simple analysis, by judiciously chosen assumptions. Final assurance of the legitimacy of the approach should be undoubtedly the pragmatic one given by close experimental checks. In the field of attack on the problem of d.c. dynamic braking of induction motors it is the way in which the saturation effects are treated, that makes the various methods of analysis differ from one another. The other assumptions such as negligible effects due to space harmonic m.m.f's and those produced by iron and stray losses, are common for all the methods. Also in all the methods, the variation of secondary resistance and reactance with the speed is neglected. The induction motor method is simple, straightforward and accurate from both theoretical and practical aspects of an ordinary induction motor under d.c. braking. The Potier triangle method can also compete with the Induction motor method of analysis though it involves a little more of simplifying assumptions. Both the methods are devoid of laborious calculations and as such convenient for use.

APPENDIX-I

DYNAMIC BRAKING OF DOUBLE CAGE MOTORS

In the double squirrel cage motor the rotor winding consists of two layers of bars short circuited by end rings. The upper bars are of small cross sectional area than the lower bars and consequently have higher resistance. The bottom cage which consists of deep bars, has relatively high inductance which is effected by properly proportioning the constriction in the slot between two bars. When the rotor current frequency is high, there is relatively little current in the lower bars because of their high reactance and hence the effective resistance of the rotor at higher frequencies approximates that of the high resistance upper cage. At low rotor current frequencies, however, reactance becomes unimportant and the rotor resistance, then approaches that of the two layers in parallel. Such a construction is adopted to achieve higher starting torques at the sacrifice of the efficiency for normal running.

In order to suit its special construction the treatment of the double cage motors for performance prediction[25], requires further modifications of the assumptions employed in the performance analysis of the ordinary induction motor. This is true both for motoring and dynamic-braking performance of the double cage motors, and is due to the fact that the various approximations incorporated in the development of the performance equations for ordinary induction motor will cause greater error in the case of these special motors for which the rotor resistance and leakage reactance vary appreciably with frequency. It is possible[25] however to adopt and extend the induction motor approach with suitable modifications.

Equivalent Circuit for normal operation.

The equivalent circuit of the double cage motors is arrived at, as in the case of single cage ones, except that in the present case the secondary part of the same has to be modified. Provided both the cages completely link the main flux they may be considered as parallel windings. Then the equivalent circuit can be represented as shown in fig. 1 where R_1, X_1, are the stator resistance and reactance, R_c represents the core loss, X_m the magnetizing reactance, X_{2c} and X'_{2i} being the resistance and reactance of the inner cage referred to the stator and R_{20}, X'_{20} being the corresponding values for the outer cage.

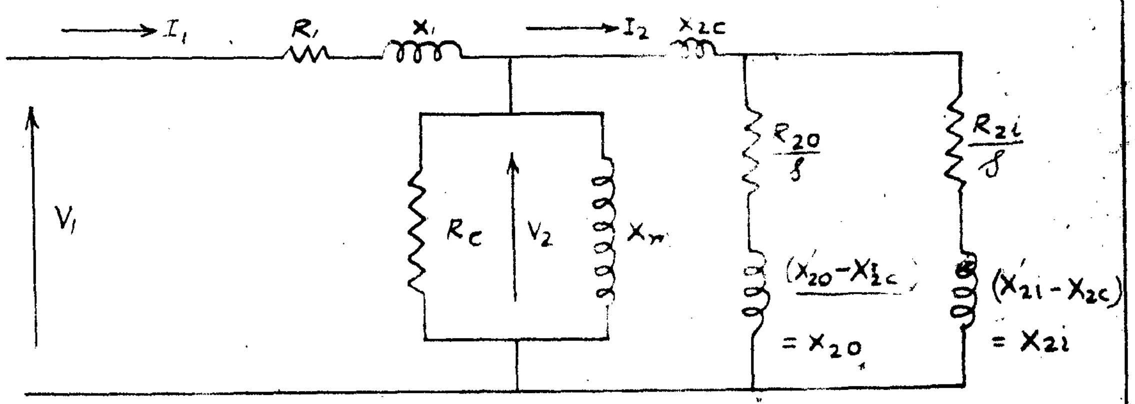

FIG. 1

EQUIVALENT CIRCUIT FOR NORMAL OPERATION OF A DOUBLE CAGE INDUCTION MOTOR.

It may again be noted that the friction, windage, and the iron and stray losses are not taken into account along with those caused by the space harmonics.

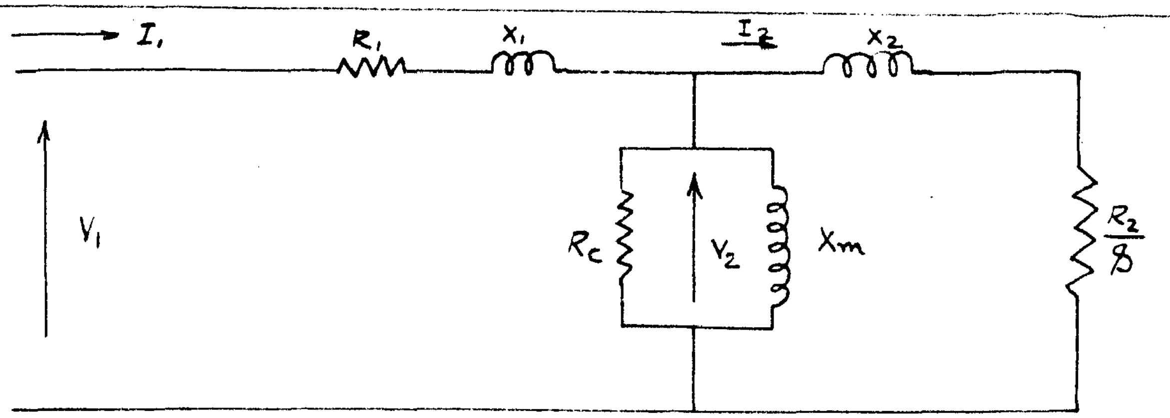

FIG. 2

EQUIVALENT CIRCUIT OF A DOUBLE CAGE MOTOR MODIFIED FROM THAT SHOWN IN FIG.

The equivalent circuit for normal operation can be further modified as shown in fig. 2. The reactance $X_{20} = X'_{20} - X_{2c}$, is negligible and is omitted, because the very construction is such that this is inherently a low value. The values of R_2 and X_2 can be easily derived[25,32] and shown to be

$$R_2 = R_{20} \left[1 - \frac{A}{1 + s^2 B^2} \right] \qquad 1$$

$$X_2 = X_{2c} + \frac{X_{21} A^2}{1 + s^2 B^2} \qquad 2$$

$$\left.\begin{array}{lll} \text{where} & A = & \dfrac{R_{20}}{R_{20} + R_{21}} \\ & & \\ \text{and} & B = & \dfrac{X_{21}}{R_{20} + R_{21}} \end{array}\right\} \qquad 3$$

Under dynamic braking conditions the equivalent circuit may be modified further as shown in fig. 2.3. As for the ordinary induction motors it is assumed that the primary current is the alternating current equivalent of the stator direct current electromagnetically, and having the normal frequency of operation $_s$. Also the various reactances referred to are based on this frequency. R_1 , X_1 and R_c need not be considered as before and are omitted. Saturation has to be accounted for, and hence adjusted values of X_m have to be used. Also the fractional or per unit frequency of the rotor induced e.m.f. being $S = \frac{N}{N_s}$, this replaces s which is the per unit frequency of rotor e.m.f. for normal operation. Hence for dynamic braking operation the equations 1 and 2 can be written down as

$$R_2 = R_{20} \left[1 - \frac{A}{1 + S^2 B^2} \right] \qquad 4$$

$$X_2 = X_{2c} + \frac{X_{2i} \quad A^2}{1 + S^2 B^2} \qquad 5$$

Substituting these values of R_2 and X_2 in equations 1.5 to 1.7, the dynamic braking torque/speed characteristics may be obtained. It may be noted that the complex variation of R_{20} and R_{2i} with the frequency cannot be taken into account in the calculations based on the equivalent circuit. The stray load losses become pronounced[25] in the double cage motors under dynamic braking. Hence it is necessary to determine the stray loss torques versus speed separately by the standard reversed rotational test[29] and superimpose the same on the torque-speed characteristic as calculated using equations 1.1 to 1.7 and equations 4 and 5.

Determination of the parameters of the equivalent circuit from test data[25, 32]

Tests can be conducted with the rotor kept at standstill and applying a variable voltage, variable frequency 3 phase supply to the stator. Then with the supply to the stator at normal frequency with the rotor kept at standstill, we have the value of R_2 given by equation 1 where $s = 1$

$$R_{2f} = \frac{R_{20} (D + B^2)}{1 + B^2} \qquad 6$$

where $$D = \frac{R_{21}}{R_{20} + R_{21}} \qquad 7$$

Also with the rotor at standstill and applying a voltage of r times the normal frequency we get

$$R_{2r} = R_{20} \frac{(D + r^2 B^2)}{1 + r^2 B^2} \qquad 8$$

Neglecting the magnetizing and core loss components of the equivalent circuit and taking the value of R_1 at its d.c. value, the value of R_{2r} can be determined at different values of r, and hence the values of D and B can be determined and an average value can be taken for calculations. Knowing D and B, R_{20}, R_{21} and X_{21} can be evaluated.

Also in a similar way the rotor reactance at a voltage of r times the normal frequency we get

$$X_{2r} = r\,X_{2c} + \frac{r\,X_{21}\,A}{1 + r^2 B^2} \qquad 9$$

Now the total reactance measured with a voltage of r times the normal frequency is given by

$$X_{tr} = r\left[X_1 + X_{2c}\right] + \frac{rX_{21}\,A}{1 + r^2 B^2} \qquad 10$$

It can be assumed that $X_1 = X_{2c}$, and hence the value of X_{2c} can be determined. The value of the magnetizing reactance X_m can now be found out by the no load test on the motor.

Nature of torque/speed characteristics of a double cage motor.

Typical torque/speed characteristics[25] of a double cage motor for both motoring and braking operation are shown in fig. 4. Curve A is for motoring operation, with normal supply voltage, and curve B shows the total torque inclusive of the stray loss torques, vs. speed for dynamic braking operation with per unit excitation $I_1 = 2.87$. The dotted lines on curve B shows the deviation if the stray loss torques are not considered. As compared to an ordinary induction motor (fig. 2.9) it is immediately clear that there is not much of a similarity of the motoring curve and braking curve for the double cage motors. It can be seen that the braking characteristic of a double cage motor is similar to that of a normal induction motor. But it may be noted that the rotor resistance of the double cage motor being 2 to 3 times more than that of a corresponding single cage motor at higher speeds, the torque will be higher in this speed range as compared to the normal induction motor.

It is evident from the torque/speed curve that it is the area under unstable speed range that will considerably affect the stopping time and as such a reasonable decrease in the stopping time can be expected from the double cage motors. A decrease to the extent of 50% is forecast[25] for a standard double cage motor. Hence with the already good starting characteristic, the double cage motors have a comparatively better braking performance and as such will be the most suitable for frequent start-stop drives as compared to the single cage machines.

APPENDIX - 2

REQUIREMENTS OF THE D.C. SOURCE AND THE DESIGN ASPECTS OF THE MOTOR FOR D.C. BRAKING

Obviously the d.c. supply should be a stable, low voltage, high current source. Many a time this is one of the disadvantages that induce the industrialists to adopt a different method of braking. But the evolution of well designed metal rectifiers with very satisfactory characteristics, has accelerated the adoption of d.c. braking schemes in many small size industrial applications.

The insulation of the direct current source should be able to withstand the residual a.c. voltage on the stator at almost 50 frequency, and sufficient care should be excercised to see that the residual voltage is not too high by giving a time lag from switching off the a.c. supply and injecting the direct current. For example for an 11-KV motor the d.c. voltage should not be switched on till the a.c. voltage has decayed to safe limits. This can be done by incorporating a suitable timer in the control system.

Also the regulation of the supply source should be capable of meeting the sudden rise of the load current to the stator winding, the rate of rise of which will be fast because of the short circuited rotor.

With regards to the design aspects it should be seen that the magnitude of the direct current and the connection used (Refer figure 1.1) should be such that overheating is avoided, at the same time meeting the requirements of the braking performance.

Referring to figure 1.1 connection(b) is preferred for star-connected stator winding even though the heating is non-uniform, because only two contacts are required for injecting d.c. whereas in connection (a) , 3 contacts are required. But in cases where the magnitude of direct current required may cause overheating, connection (a) is invariably used. Also it may be noticed that in connection (b) a higher voltage direct current source can be used. For delta -connected stator windings connection (c) is invariably used because it gives more uniform heating of the windings with a simpler control scheme.

Regarding motor itself, all the mechanical parts subject to reversing stresses are to be liberally dimensioned to safely withstand the reversed peak torque during braking. The rotor design should be mechanically sound and special attention is to be paid for cage rotor bars and end rings. The insulation of the rotor winding should be able to withstand the high induced e.m.f. obtained with values of excitation 3 to 4 times the rated current. The stator winding has also to be well braced. All the above requirements are dependent upon the type of application and therefore cannot be strictly generalised.

BIBLIOGRAPHY

1. " Bremsen von Induktionsmotoren mittels Gleichstrom"
   Hellmond R.E. Electrotechnik and Maschinenbau 1910, 28,p.837.

2. Improvements in braking Induction motors
   Rosenberg. E. and Peck J.S. British patent application No.17010, 1910.

3. "Die Asynchronmachine mit Gleichstrom Erregt als Bremse"
   Weissheimer.H.Archiv fur Electrotechnik 1934, 28,p.487.

4. "D.C. braking of Induction Motors.
   Harrel F.E. and Hough W.R. Transaction A.I.E.E, 1935, 54,p.488.

5. Discussion on the above.
   Hellmond Ibid 1936, 55, p.168.

6. Dynamic braking of A.C. winders.
   Worrel R.W. Metropolitan Vicker's Gazette 1938,17,p.239.

7. Comparison of methods of stopping squirrel cage motors
   Bendz W.I. Trans. A.I.E.E, 1938, 57, p.499.

8. Dynamic braking.
   Millar.T. Electrical Review 1943, December p.887.

9. Principles and features of a new dynamic braking and motor control system for A.C. winders.
   Friedlander,E; G.E.C. Journal 1949, 16, p.204.

10. Dynamic braking of Induction motors.
    Watts C.B. Electrical times 1950, 118, p.136.

11. The dynamic braking of alternating current motors
Harrison. D. Engineering 1950, 170, p.528.

12. Equivalent circuits of electric machinary
Kron, (Book) John Wiley 1951.

13. D.C.Dynamic braking of squirrel cage motors
LaPierre.W. and Metaxas. N; Trans. A.I.E.E, 1953,72,p.981.

14. Discussion on above.
Rosenberry G.M.; Ibid p.984.

15. Calculation of dynamic braking characteristics of wound rotor Induction Motors.
Cochran P.L; Ibid 992.

16. Dynamic braking of slip-ring Induction Motors applied to mine winders.
Mulligan J.W. Metropolitan Vickers Gazette 1953, 24,p.375.

17. Some experiences in the dynamic braking of a.c. winders
Powell D.W. and Williams. H.; Mining electrical and mechanical engineer 1953, 33, p.351-67, 391-402.

18. Dynamic braking of squirrel-cage Induction motors.
Evert. C.F. Trans. A.I.E.E. 1954, 78, p.242.

19. Calculation of maximum torque and critical slip in the dynamic braking of Induction motors.
Stulnikov V.I, Archiv fur Electrotechnik 1954,28,p.487.

20. The dynamic braking of Induction motors.
Harrison D. Proceedings I.E.E, 1955, 103 A, p.121.

21. Discussion on Ref.20.
Butler O.I. Ibid p.129.

22. The effect of magnetic saturation on the D.C. Dynamic braking characteristics of A.C. motors.
Butler O.I. Ibid, monograph Nov. 1956.

23. A two motor A.C. mine hoist control system.
Myles, Trans. A.I.E.E. 1956, 75, p.10-16.

24. Stopping time and energy losses of A.C. motors with D.C. Braking.
Butler O.I.; Ibid, 1957, 76, p.285.

25. D.C. Dynamic braking of double cage Induction motors.
Butler O.I., Abdel Hamid M.N; Trans. A.I.E.E; 1958, 77,p.1035.

26. A.C. motor control.
Watts J.C; Electrical Review 1957, 161, p.1169.

27. Dynamic braking of A.C. mine winders.
Petch T.H; Thomas. D, BTH activities 1958,29,p.207.

28. Induction motor characteristics at high slip.
Theodore. H.Morgan, Brown.W.E. Trans. A.I.E.E,1940,59, p.464.

29. Reversed rotation test for the determination of the Stray load loss in induction machines.
Morgan. T.H., Brown W.E., Schumer.A.J., Ibid 1939,58, p.319.